A Thesis for the Degree of Master of Engineering

Development of a Natural Calcium Phosphate Biomaterial Using Horse Bones

말 뼈를 이용한 천연 인산칼슘계 생체소재 개발

CHO, WOO JAE

조 우 재

February 2014

Department of Biosystems & Biomaterials Science and Engineering

Major of Biosystems Engineering

The Graduate School

Seoul National University

Seoul National University

Development of a Natural Calcium Phosphate Biomaterial Using Horse Bones

말 뼈를 이용한 천연 인산칼슘계 생체소재 개발

지도교수 정 종 훈

이 논문을 공학석사학위논문으로 제출함

2014년 2월

서울대학교 대학원

바이오시스템◦소재학부 바이오시스템공학 전공

조 우 재

조우재의 석사학위논문을 인준함

2014년 1월

위 원 장 김 용 노 (인)

부 위 원 장 정 종 훈 (인)

위 원 김 학 진 (인)

Development of a Natural Calcium Phosphate Biomaterial Using Horse Bones

Cho, Woo Jae

Department of Biosystems & Biomaterials Science and Engineering

Major of Biosystems Engineering

The Graduate School

Seoul National University

Abstract

Calcium phosphate is main component of hard tissues of the human body such as teeth and bones. For this reason, calcium phosphate has been studied for the medical application (e.g. dental fillers, bone scaffolds, and bone cements). In particular, it was reported that hydroxyapatite (HA, $Ca_{10}(PO_4)_6(OH)_2$), which is a type of calcium phosphate, had some useful properties such as high biocompatibility, bioactivity, osteoconductivity, osteoinductivity, nontoxicity, and low immunogenicity, etc. Also, it has been widely known that biowastes such as porcine bones, bovine bones, fish scale, and fish bones could be used as raw materials for production of HA with their low prices and large scale production. However, horse bones were seldom used as a bioresource for the production of

natural hydroxyapatite, and the production process was not constructed despite the increase of their production, low price, and free of foot-and-mouth disease.

This research was carried out to suggest an optimized process for the production of a new natural calcium phosphate biomaterial using horse bones. The initial production process was referred to the previous method which was constructed for the porcine bone powders (immersion in for H_2O_2 for 48 h, sintering at 1200 ℃ for 16 h, and grinding). The characteristics of horse bone-derived calcium phosphate biomaterials were investigated according to the different osseous tissue types (i.e., compact bone and cancellous bone), bone types (i.e., spine and tibia), pretreatment methods (cold water, H_2O_2, and hot water), sintering time, and sintering temperature. In addition, for more wide medical application, the resultants should be made as a powder type, so the grinding methods were compared based on the wet grinding (ball mill) and dry grinding (blade grinder). For the evaluation of the potential of horse bone powders processed as a biomaterial, cell *in vitro* test was carried out using the MC3T3-E1 cells with the synthetic HA and commercial bovine bone materials (Bio-Oss). The obtained horse bone powders were characterized by thermal gravimetric analysis (TGA), X-ray diffraction analysis (XRD), Fourier transform infrared spectroscopy (FT-IR), X-ray fluorescence spectrometry (XRF), and field emission scanning electron scanning microscopy (FE-SEM). The results showed that there were no significant differences according to the types of osseous tissue and bone. Also, the pretreatment methods did not influence to the resultants, but considering the processing time, hot water method was selected. And the sintering time was enough for 12 h. There were many differences according to the sintering temperature, The XRD peak of horse bone

sintered at 600℃ was most close to the HA, but horse bone sintered at 1100℃ was the best in cell toxicity and horse bone sintered at 1300℃ showed the best cell proliferation *in vitro* test.

This research showed that the horse bone could be a promising resource for the natural calcium phosphate biomaterial and horse bone powders had a great potential as biomaterials for bone tissue engineering.

Key words: bone substitute, horse bone, bone powders, calcium phosphate biomaterial, natural hydroxyapatite, bone tissue engineering.

Contents

List of Figures

List of Tables

List of Terms and Abbreviations

HA	hydroxyapatite
TGA	thermal gravimetric analysis
XRD	X-ray diffraction analysis
FT-IR	Fourier transform infrared spectroscopy
XRF	X-ray fluorescence spectrometry
FE-SEM	field emission scanning electron scanning microscopy
β-TCP	β-tricalcium phosphate
P(D,L)LA	poly-D,L-lactic acid
MSCs	mesenchymal stem cells
CW	cold water method
HW	hot water method
FBS	fetal bovine serum
PDMS	polydimethylsiloxane
HMDS	hexamethyldisilazane
SAS	statistical analysis system
HB	horse bone

1. Introduction

Tissue engineering is defined as an interdisciplinary field that applies the principles of engineering and the life sciences toward the development of biological substitutes that restore, maintain, or improve tissue function [1, 2]. In recent years, the importance of bone tissue engineering has grown as the number of bone defects and bone fracture has increased due to the aging society. It was well known that people showed loss of density and strength with age [3]. Indeed, Johnell and Kanis reported that there were 9.0 million patients worldwide only in the osteoporotic fractures in 2000 [4]. Accordingly, in bone tissue engineering, bone replacement grafts have emerged for bone reconstruction and bone healing. Various materials are available for grafting, and they are usually classified four groups: autograft, allograft, xenograft, and alloplast. Autograft is the bone graft using the autogenous bone. It is the most effective bone graft material in osteointegration, osteoconduction, osteoinduction, and osteogenesis. Allograft is the next best alternative bone graft material, which uses the bones from the same species. However, they have some limitations such as the obtainable quantities limit, high cost, complex surgical procedure, immune reaction and the risk of infection [5, 6]. Alloplast uses the synthetic graft material such as bioglass and glass ionomer, etc. It has potential to offer not only the advantages of autograft and allograft, but also the various bioactive modifications. Alloplast is a complex and comprehensive group because the base materials could be derived from other graft materials. So, it would not be discussed in this thesis. Xenograft uses the materials from different species like bovines or porcines. So it is easy to obtain and the cost of raw materials is cheap. However, xenograft has some limitations such as the immune reaction

or the risk of infection. To overcome its limitations, Ueno et al. sintered a bovine bone and used it as a new bone substitute [7]. After this study, Taniguchi et al. conducted surgical implantation using the sintered bovine bone and reported that infection or fracture was not observed [8]. From these results, the sintered bones have a potential as a suitable material for bone substitute to provide bone regeneration and promote bone healing. In particular, it was reported that the sintered bovine bones were mainly composed of hydroxyapatite (HA). Human bones also consisted of organic (30%) and inorganic compounds (70%), and inorganic compounds, which were predominantly composed of HA [6, 9]. From these results, we concluded that we could obtain calcium phosphate biomaterials by sintering the bioresources such as animal bones or teeth. Although calcium phosphates including HA can be manufactured synthetically, natural calcium phosphates have the advantages of low production cost, cheap raw material and better biological properties [10, 11]. Therefore, various biomaterials from bioresources have been developed. For example, porcine bones [9, 12, 13], bovine bones [7-9, 11, 14, 15], chicken bones [16], and fish bones and scales [17, 18] were reported as useful bioresources for natural calcium phosphate. However, horse bone has been overlooked despite the potential as a bioresource for manufacturing the natural calcium phosphate biomaterials. Kim et al. reported that the number of horse slaughter in Korea was increased [19]. Accordingly, the biowastes from horse would be increased. In this respect, the horse bones have a great potential as a new bioresource for natural calcium phosphate biomaterials.

In this thesis, natural calcium phosphate materials derived from horse bones were developed and evaluated to verify the potential as a new bioresources for calcium

phosphate materials using physiochemical characterizations [13, 15, 16, 20, 21] and biological studies [10, 12, 14], with the control groups: calcium phosphate derived from bovine bone; Bio-Oss (Geistlich Biomaterials, Switzerland); synthetic HA (#289396, Sigma Aldrich, USA). In detail, it was reported that the HA derived from biowastes could be influenced by some conditions, such as the types of osseous tissue (i.e. compact bone and cancellous bone) [22] and bone (tibia and spine) [9, 23], pretreatment methods [9, 15], and sintering conditions [24, 25]. However, the previous study overlooked these variables and the main target was porcine [12, 26]. Therefore, for the optimization of the production process of calcium phosphate biomaterials derived from horse bone, various factors (the types of osseous tissue and bone, pretreatment methods, sintering time, and sintering temperature) were examined. For physiochemical characterizations, the sintered horse bone powders were characterized by thermal gravimetric analysis (TGA), X-ray diffraction analysis (XRD), Fourier transform infrared spectroscopy (FT-IR), X-ray fluorescence spectrometry (XRF), and field emission scanning electron scanning microscopy (FE-SEM). And, for cell proliferation and cell cytotoxicity study, MC3T3-E1 which was well known for as an *in vitro* model of osteoblast development [27, 28] was used. In addition, the horse bones were ground into powders for the extensive application, such as mixing materials for scaffolds or bone cements. For this, two types of grinding, a ball mill (wet) and a blade grinder (dry) were tested and investigated using a particle size analyzer (Mastersizer S, Malvern Instruments Ltd, UK)

2. Objectives

The objective of this thesis was to develop a new calcium phosphate biomaterial using sintered horse bone. For this, the methodologies for the production of the natural calcium phosphate derived from horse bones were needed and the optimized production process were required. Based on these results, the possibilities of the developed calcium phosphate as a biomaterial were examined.

Detailed objectives were as follows:

1) To develop and optimize the methodologies for the production of a new calcium phosphate biomaterial using sintered horse bones.

2) To investigate the characteristics of the developed calcium phosphate biomaterials and evaluate their biocompatibility.

3. Literature Review

3. 1. Calcium phosphate materials as bone substitutes

In 1920, Albee used the first calcium phosphate materials in tissue engineering applications. They used “tri-calcium phosphate” compounds in surgically created bone defects in rabbits and reported the promoted bone formation [29]. In 1951, Ray and Ward Jr reported the effect of a granular synthetic HA in bone replacement [30]. Subsequent to these studies, initial studies with attempts to better understand the calcium phosphate materials were carried out. In 1971, Monroe et al. fabricated white translucent polycrystalline ceramic from synthetic hydroxyapatite and suggested its use for dental or medical implant based on the similarities among the mineral compositions of bone and teeth and this ceramic [31]. In the next year, 1972, Getter et al. selected three calcium phosphate compounds (monocalcium phosphate, dicalcium phosphate, and β-tricalcium phosphate (β-TCP)) and confirmed β-TCP was the most effective implant material in the *in vivo* experiment in rats and rabbits [32].

3. 2. Hydroxyapatite

In 1957, Fernandez-Moran and Engstrom investigated the bone sections using electron microscope and X-ray diffraction [21]. They showed the apatite particles were adsorbed to the collagen fibers in a highly ordered way and demonstrated the existence of crystalline hydroxyapatite. In 1976, Jarcho et al. suggested a new process for dense, polycrystalline hydroxyapatite close to theoretical density and is free of fine pores and second phases [33].

In 1980, de Groot assumed the bone mineral would be hydroxyapatite, based on the molar ratio Ca to P [34]. He reported that the synthesized calcium phosphate could compete with autologous bone in animal and clinical studies. Besides these studies, many other studies were carried out related to the HA and the results suggested the merits of HA, such as bioactivity, biocompatibility, osteoconductivity, non-toxicity, noninflammatory and nonimmunogenic reaction. Consequentially, HA has attracted considerable attention and HA is still widely studied and utilized in bone tissue engineering.

3. 3. Advantages of natural HA

In accordance with the increased interests in HA, a number of techniques have been suggested for producing HA. These techniques could be categorized into two types: derived from natural sources or from synthetic sources [9]. It was reported that natural HA derived from animal bone has some advantages. In 1999, Matsumoto et al. compared the effects of sintered bovine bone and synthetic hydroxyapatite-based material regarding the DNA and collagen synthesis and osteoblastic expression in osteoblast-like cell [35]. They reported that the sintered bovine bone (i.e. natural HA) showed better results in the synthesis of DNA and collagenous protein, the proliferation and differentiation of osteoblast-like cells., and the alkaline phosphatase activity. Subsequently, in 2000, Guizzardi and his colleagues carried out *in vitro* study and *in vivo* study using the natural apatite derived from the horse compact bone and synthetic porous HA [10]. In this study, natural apatite showed better bone ingrowth *in vivo* and stimulated proliferation and alkaline phosphatase activity *in vitro*. In 2009, Mezahi et al. studied the dissolution kinetic and structural behavior of natural HA

and synthetic HA by the observation of Ca and P concentrations in the SBF solution [11]. They reported that the dissolution was occurred more in N-HA than in S-HA and the formation of new phosphate phase was also more in N-HA than in S-HA. The comparison between natural HA and synthetic HA were shown in table Ⅰ [36].

Table I. Comparison between natural HA and synthetic HA

Source	Advantages	Disadvantages
Natural source	Abundant source Relatively low requirement for equipment Relatively low cost Natural architecture preservation	Variation of resultant properties Collection of biowastes
Synthetic source	Pure resultant Manageable conditions Reproducibility	Residual chemical and organic components Time consuming Less osteoconductive properties Less dissolution

3. 4. Sintered bone as sources of natural HA

In 1983, the utilization of biowastes as bone substitutes were reported by Ueno and his colleagues [7]. They developed sintered cancellous bovine bone as a bone substitute. The process for the sintered bone was involved boiling raw bone for 10 h, pretreatment with 1 % H_2O_2 and 1 % NaOH, neutralization with 1N HCl, and finally, sintering first at 600°C for 3 to 5 h, next, heating for 3 h with increasing the heating temperature from 600°C to 1100°C was followed and the heating in 1100°C was lasted for 3 h. Subsequent to the development of the sintered bovine bone, Taniguchi et al. treated the 22 patients who had benign bone tumors in the hand with the developed sintered bovine bone, and reported bone union was observed in all patients without any other abnormal findings in 1999 [8]. Up to this time, bovine bones have been attractive resources due to the popularity as food and the similarity in bone composition to human bone. In 2006, Danilchenko et al. made two bone samples, in solid form and in powder form and observed the thermal behavior of samples by X-ray diffraction [25]. And, Ooi et al. (2007) [24] and Barakat et al. (2008) also produced natural HA by sintering of bovine bone. Ooi et al. showed that the residual protein of bovine bones could be removed by sintering, and bovine bones annealed between 700 and 1200℃ exhibited a form of HA and a high degree of crystallization at high temperature above 1000℃. Barakat et al. compared three methodologies respectively using the subcritical water, alkaline hydrolysis, and calcination (sintering) for extraction of natural hydroxyapatite bioceramic from bovine bone. They reported the production of carbonated hydroxyapatite or carbonate-free hydroxyapatite.

In 2008, Janus et al. investigated the chemical and microstructural characteristics of natural

hydroxyapatite derived from pig bones, and reported the reduced Ca/P ratio after heat treatment [13]. In previous study of our laboratory, Im et al. (2007) fabricated a composite scaffold consisted of poly-D,L-lactic acid (P(D,L)LA) and bioceramic materials derived from pig bone powders [12]. They tested the cell cytotoxicity of the composite scaffold using the dental pulp stem cells.

Besides the bones derived from vertebrates, biowastes from fishes were reported as new sources for biomaterials. In 2002, Ozawa and Suzuki proposed the natural hydroxyapatite originated from fish bone waste through the heat treatment at temperatures <1300°C and reported that the fish bone heated at 1300°C became a hydroxyapatite ceramic with a tricalcium phosphate (TCP) phase [17]. In 2012, Mondal et al. collected fish scales from fresh water fish (Labeo rohita) and de-proteinized with the HCL solution for 24 h and after sintering, extracted hydroxyapatite powders [18]. Preparation methods and raw materials of natural calcium phosphate were shown in table Ⅱ.

Table II. Preparation of natural calcium phosphate with thermal treatment

Authors	Raw material	Pretreatment	Temperature (℃)	Annealing time
Ueno et al. [7] and Taniguchi et al. [8]	Bovine bone	Boiling; 1 % H_2O_2 and 1 % NaOH	1100	3 h
Ooi et al. [24]	Bovine bone	Not mentioned	400, 500, 600, 700, 800, 900, 1000, 1100, 1200	2 h
Danilchenko et al. [25]	Bovine bone	Not mentioned	100, 600, 700, 800, 900, 1000, 1100, 1300	45 min
Janus et al. [13]	Porcine bone	Boiling; Leaching in NaOH	800, 1200	Not mentioned
Im et al. [12]	Porcine bone	H_2O_2	1200	6 h
Baik et al. [26]	Porcine bone and horse bone	H_2O_2	1200	16 h
Ozawa et al. [17]	Fish bone	Boiling	600, 800, 1000	1 h
Mondal et al. [18]	Fish scale	Deproteinization in 1 (N) HCl 35% solution (2:1, v/w, water HCl /fish scale)	1100	2 h

These results suggested that animal bones could be good sources for natural calcium phosphate materials.

3. 5. Characterization and production process of natural HA

Thermal treatment (i.e. sintering) was the representative method for manufacturing the natural HA. Thermal treatment could remove the organic compounds such as collagen, laminin, and fat with a simple procedure, relatively low requirement in equipment and the low risk in disease transmission of the resultant [36]. Specifically, thermal treatment could preserve the natural bone architecture closely resembling that of the bone from which it was produced [7, 23, 35]. For these reasons, the production process in this thesis was achieved based on thermal treatment.

The final resultant of this study was made as a powder type. Because, powder typed HA could be easily adapted to other bone substitute materials such as bone scaffolds, bone fillers or bone cements. Also, it was reported that the powder size of the HA could influence to the bioactivity [37-40]. In 2006, Cai et al. investigated the effects of nano HA particles with 20, 40 and 80 nm diameter, on the proliferation of two bone-related cells, bone marrow mesenchymal stem cells (MSCs) and osteosarcoma cells (U2OS) [37]. They reported that the cell viability and proliferation of MSCs were improved and the growth of osteosarcoma cells was inhibited *in vivo*, specifically in 20 nm. Subsequently, Shi et al. (2009) compared the size effects on the proliferation of human osteoblast-like MG-63 cells with nano HA particles (20 nm and 80 nm) and micro HA particles [38]. They also reported that Np20 had the best effect on promotion of cell growth and inhibition of cell apoptosis. And, in 2010, Yuan et al. investigated the effect of the particle size of the HA on the anti-tumor activity using human hepatoma HepG2 model cells [39]. Their results showed that the anti-tumor activity and induced apoptosis were occurred in HepG2 cells, and the effects were

decreased in the order of 45 nm> 26 nm > 78 nm > 175 nm. These results suggest the benefits of nano HA powders. So, in this thesis grinding and milling were adapted to the sintered animal bones for the production of nano size powders.

As mentioned, the species of raw materials or the type of bone [9, 23], pretreatment methods [9, 15], and sintering conditions [24, 25] could influence the resulting HA. This was the first study to develop a bone substitute using the horse bone as a resource for natural HA. So the effect of the type of bone was examined using the same process in previous study [12] with the bone types (i.e., spine and tibia) and osseous tissue types (i.e., compact bone and cancellous bone). And, pretreatment methods were examined with three conditions: immersion in cold water, H_2O_2, and boiling water. There were two factors in sintering process: temperature and time. The sintering temperature were selected based on the preceding TGA results. Characterization of each resultant was accomplished using X-ray diffraction analysis (XRD), Fourier transform infrared spectroscopy (FT-IR), X-ray fluorescence spectrometry (XRF), and field emission scanning electron scanning microscopy (FE-SEM), based on the previous studies [9, 12, 13, 15, 17, 18, 20, 23-25].

For biocompatibility, *in vitro* cell studies (cell proliferation test and cell cytotoxicity test) were carried out. As control groups, bovine bones from Korean native cattle, Bio-Oss (Geistlich Biomaterials, Switzerland), and synthetic HA (#289396, Sigma Aldrich, USA) were selected.

4. Materials and Methods

4.1. Preparation of horse bone powders

Horse bones were originated from the slaughter house in Jeju, Korea and initially cut into pieces with approximately 2~3 cm to put the pieces into the crucible. For the next step, the bone pieces were soaked in distilled water for 48 h to drain blood and cut out flesh on the surface. This process was adapted in common.

4.2. Characteristics according to the types of osseous tissue and bone

After the common process, the traditional preparation process used for porcine bones in previous study [12, 26] was carried out. Briefly, the bone samples were initially prepared according to the bone types (i.e., spine and tibia) and osseous tissue types (i.e., compact bone and cancellous bone). The bone samples were immersed in H_2O_2 (#7722-84-81, Duksan chemicals co., Korea) for 48 h and dried. After the drying, the animal bones were sintered in the electric furnace (UP350E, Yokogawa Co, Japan) at 1200℃ for 2 h. And then, the sintered bone was ground into powder with using a miller (A10, IKA, Germany), and the bone powders were sintered two times more as described before. The animal bone powder was classified in a particle size of below 100 μm with sieves (Daihan Scientific, Korea). The comparison of the resultant from the each pretreatment method was accomplished based on the results of the FT-IR, XRD, and XRF.

4.3. Characteristics according to the pretreatment methods

After the common process, three different pretreatment methods were adapted: immersion in (1) cold water, (2) H_2O_2, and (3) hot water. Each conditions were described as follows.

(1) Cold water method (CW): The animal bones after the common process were immersed in water with the room temperature for 48 h.

(2) H_2O_2 method: It was the same method in previous study reported by Im et al. (2007) [12]. Briefly, the animal bones after the common process were immersed in H_2O_2 (#7722-84-81, Duksan chemicals co., Korea) for 48 h.

(3) Hot water method (HW): The animal bones after the common process were immersed in boiling water at 1 atm for 2 h.

After the each pretreatment method, for the comparative study for the different pretreatment methods, the same process described before was used. The comparison of the resultant from the each pretreatment method was accomplished based on the results of the FT-IR, XRD, and XRF.

4.4. Characteristics according to the sintering conditions

Besides the bone types and pretreatment methods, the sintering temperature and time were verified to optimize the production process of natural calcium phosphate derived from horse bones. Based on the TGA results, the sintering temperature was selected: 600℃, 900℃, 1100℃, and 1300℃ (the reason was discussed in the results & discussion). For the

selection of the sintering time enough to remove the organic compounds, the sintering process was carried out at 600℃ with 3 steps, and the period of each step was 4 h. After the characterization, physiochemical analysis, and *in vitro* study, the optimized production process was proposed based on the results.

All of the sintering process were carried out using the alumina crucible with 10 cm * 10 cm * 5 cm (width * depth * height). And, the weight of samples was usually about 85 g.

4.5. Characterization and physiochemical analysis

4.5.1. Thermal gravimetric analysis (TGA)

The thermal gravimetric analysis of the horse bone was carried out to observe the thermal changes of horse bone according to the temperature using a thermal gravimetric analyzer (SDT Q600, TA Instruments, USA) over a temperature range of 25–1,300℃ at a heating rate of 10℃/min.

4.5.2. Fourier transform infrared spectroscopy (FT-IR) and X-ray diffraction analysis (XRD)

FTIR was measured to confirm the presence of anions partially substituting PO_4^{3-} and OH^- groups and the elimination of organic compounds. Transmission IR spectra were recorded from 4000-650 cm^{-1} with a resolution of 8 cm^{-1} using a FT-IR spectrometer (Nicolet 6700, Thermo Scientific, USA). XRD was used to examine the crystal structure of the sintered animal bone powders and other control groups. The XRD patterns were recorded with a

powder X-ray diffractometer (D8 ADVANCE with DAVINCI, Bruker, Germany) with Cu-Kα radiation (λ=0.154 nm) at 40 kV and 40 mA. Scans were obtained from 20 to 60 degrees two theta in 1 degree/min. The crystalline phase compositions were identified with reference to standard JCPDS cards available in the system software. Additionally, crystal sizes were determined from

X-ray diffraction spectra using the TOPAS software (Bruker, Germany).

4.5.3. X-ray fluorescence spectrometry (XRF)

XRF (S4 PIONEER, Bruker AXS, Germany) was used to obtain the elemental chemical composition of the sintered animal bones and control groups. It was also for the verification of the Ca/P molar ratio according to the sintering temperature,

4.5.4. Morphologic observation

The surface morphologies of the resultants and control groups were observed using a field-emission scanning electron microscope (FE-SEM) (SUPRA 55VP, Carl Zeiss, Germany).

4.6. Fine powder production

For the fine powder production, the two types of grinding (ball mill and blade grinding) were compared. As a ball mill, Planetary Mono Mill PULVERISETTE 6 classic line (Fritsch, Germany) was used. As a blade grinder, air leading grinding machine (ALG-2, Mill Powder Tech, Taiwan) was used. The particle sizes of the animal bone powders were

checked using a particle size analyzer (Mastersizer S, Malvern Instruments Ltd, UK) and FE-SEM.

Fig. 1. Two types of grinding machine. (A) Blade grinder (dry grinding, ALG-2) and (B) Ball mill (wet grinding, Planetary Mono Mill PULVERISETTE 6 classic line).

4.7. *In vitro* test

4.7.1. Cell culture

A mouse calvaria-derived osteoblast cell line, MC3T3-E1 (CRL-2593, ATCC, USA) was cultured in proliferation media. The proliferation media was alpha MEM (#LM 008-02, WELGENE Inc., Korea) supplemented with 10% fetal bovine serum (FBS, #SH30919.03, Hyclone, USA), 1% antibiotics (#LS 203-01, WELGENE Inc., Korea) at 37℃ in 5% CO_2 conditions. The media was changed every other two days.

4.7.2. Cell toxicity test

Cell cytotoxicity was assessed with an EZ-Cytox cell viability assay kit (#EZ3000, Daeillab Service Co., Korea) according to the protocol given in the instructions. For the

cell cytotoxicity test, the extraction media were prepared by immersion of the samples in the proliferation media for 24 h. 1 x 10^4 cells in 100 μL of culture media were seeded in a 96 well plate with the extraction media in triplicate and incubated at 37℃ in 5% CO_2 conditions. After 24 h of cell seeding, the media were changed and 10 μL of the EZ-Cytox reagent was added. After 2 h incubation at 37℃ in 5% CO_2 conditions, the optical densities of the plates were analyzed by a microplate absorbance reader (Sunrise, Tecan, Australia) at 450 nm.

4.7.3 Cell proliferation test

Animal bone powders and the control groups were coated on the surface of a 24 well plate with the polydimethylsiloxane (PDMS, SYLGARD 184 SILICONE ELASTOMER KIT, Dow Corning, USA) in triplicate. After the coating, 3 X 10^4 cells were seeded on each well and incubated for 1, 4, and 7 days, and the media was changed every other two days. For cell viability test, an EZ-Cytox cell viability assay kit (#EZ3000, Daeillab Service Co., Korea) was used. After the incubation of 1, 4, and 7 days, the media were changed and 500 μL of the EZ-Cytox reagent was added. After 2 h incubation at 37℃ in 5% CO_2 conditions, the optical densities of the plates were analyzed by a microplate absorbance reader (Sunrise, Tecan, Australia) at 450 nm.

For morphological observation of the cells on the coating, 6 X 10^4 cells were seeded on the coated 24 well plate and incubated for 1 day at 37℃ in 5% CO_2 conditions.

And then, 2 mL of modified karnovsky's fixative solution was filled in the 24 well plate and stored for 2 h at 4℃ for primary fixation. The primary fixing solution was then

removed, and the cultured bone cement specimens were washed with 0.05M sodium cacodylate buffer three times at 4℃ for 10 min. The specimens were soaked in 2 mL of 1% osium tetroxide solution for 2 h for post fixation. After the solution was removed, the plate was washed two times briefly with distilled water at a room temperature. The specimens were dehydrated in 30, 50, 70, 80, 90, and 100% ethanol at room temperature for 10 min, respectively. After soaking in hexamethyldisilazane (HMDS) for 15 min two times for drying, FE-SEM analysis was carried out with a Zeiss Supra 55VP field-emission scanning electron microscope.

4.8. Statistical data analysis

Statistical analysis was carried out using the statistical analysis system (SAS) for Windows v9.3 (SAS Institute, Inc., USA). Statistical significance between control and treatment groups was compared with two-way ANOVA at *$p<0.05$. The data were reported as the mean ± standard deviation, n=3.

5. Results and Discussion

5.1. Characteristics according to the types of osseous tissue and bone

5.1.1 FT-IR

The FT-IR bands of the samples from compact bone and cancellous bone is shown in Figure 2.

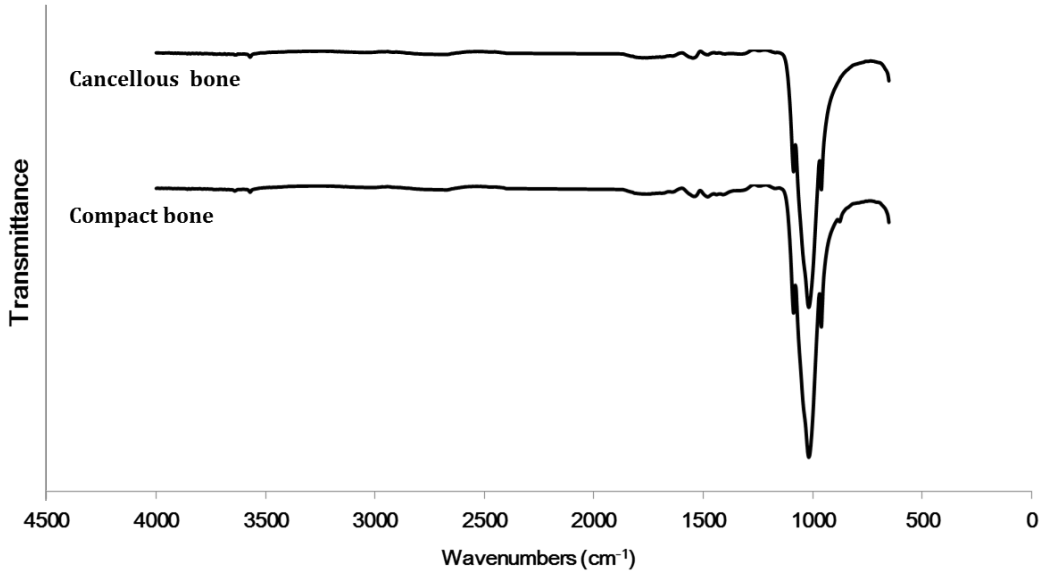

Fig. 2. FTIR spectra according to the types of osseous tissue.

There were weak bands around at 3567 cm^{-1} and 1540 cm^{-1}, and strong bands around at 1089 cm^{-1}, 1014 cm^{-1}, and 960 cm^{-1}. The band around at 3567 cm^{-1} was due to the O-H stretch of the OH group in the hydroxyapatite. The bands around at 1540 cm^{-1} indicated CO_3^{2-} originating from the mineral constituent present in the sample. The bands around at

1089 cm^{-1}, 1014 cm^{-1}, and 960 cm^{-1} indicated the PO_4^{3-} [23]. The FT-IR results showed there were same bands in compact bone and cancellous bone.

The FT-IR bands of the samples from spine and tibia is shown in Figure 3. Almost same bands with the compact bone and cancellous bone were shown, but the FT-IR spectra from the spine sample showed the absence of the bands around at 3567 $cm^{-1}$and 1540 cm^{-1}. However, the bands around at 3567 $cm^{-1}$and 1540 cm^{-1} were showed weak intensities, so it would be attributed to the small amounts of the band groups.

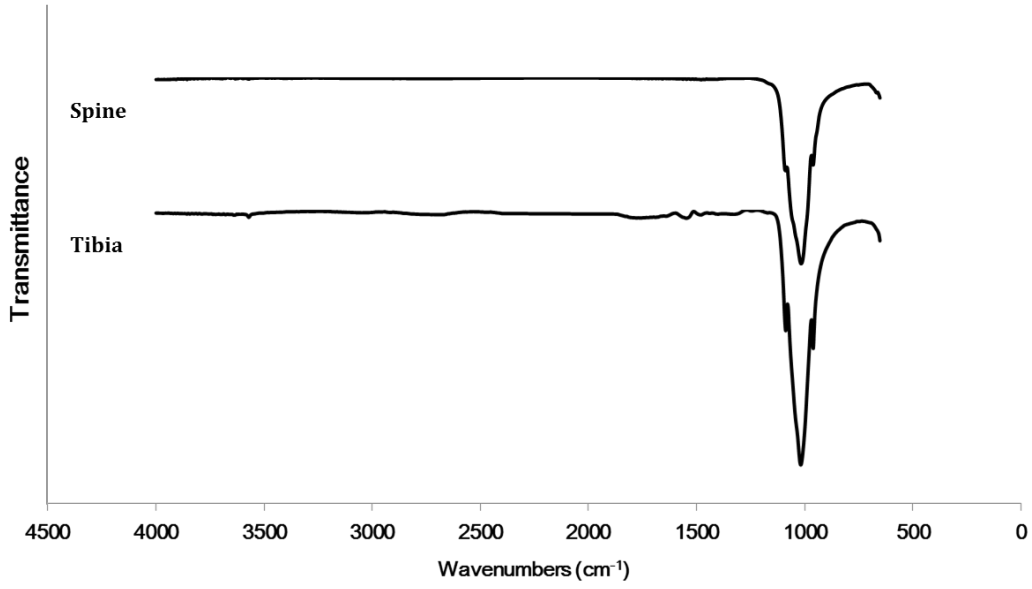

Fig. 3. FTIR spectra according to the types of bone.

5.1.2 XRD

XRD analysis of the samples were displayed with the XRD results of the synthetic hydroxyapatite as a control. Figure 4 showed the XRD patterns of the osseous tissue types. The patterns of the compact bone and cancellous bone showed the presence of peaks in

same 2θ. Also, most of their patterns corresponded to the patterns of the synthetic HA. However, there were small peaks at 37° 2θ, which indicated the presence of CaO. The presence of CaO in sintered bone was already reported by Rodrigues in 2003 [41], so the results were matched with the report.

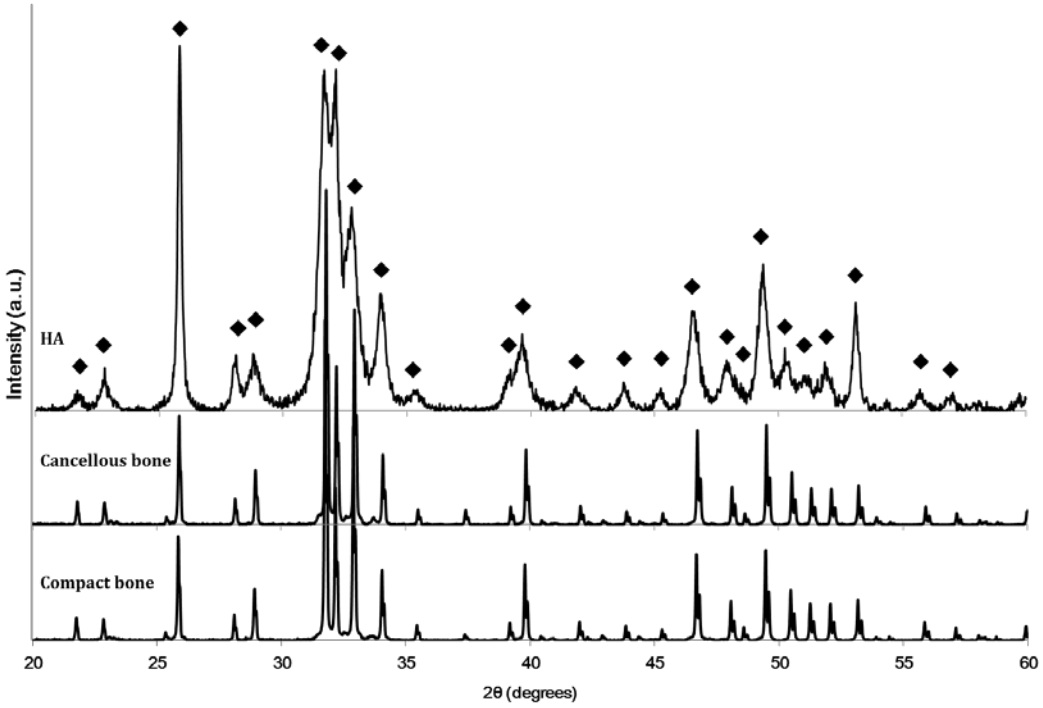

Fig. 4. XRD patterns according to the osseous tissue types and synthetic HA. (◆: Characteristic peaks of hydroxyapatite)

Figure 5 showed the XRD patterns of the bone types. The results were almost same with the patterns of the osseous tissue types. Almost same with the peaks of synthetic HA and the peaks of CaO appeared.

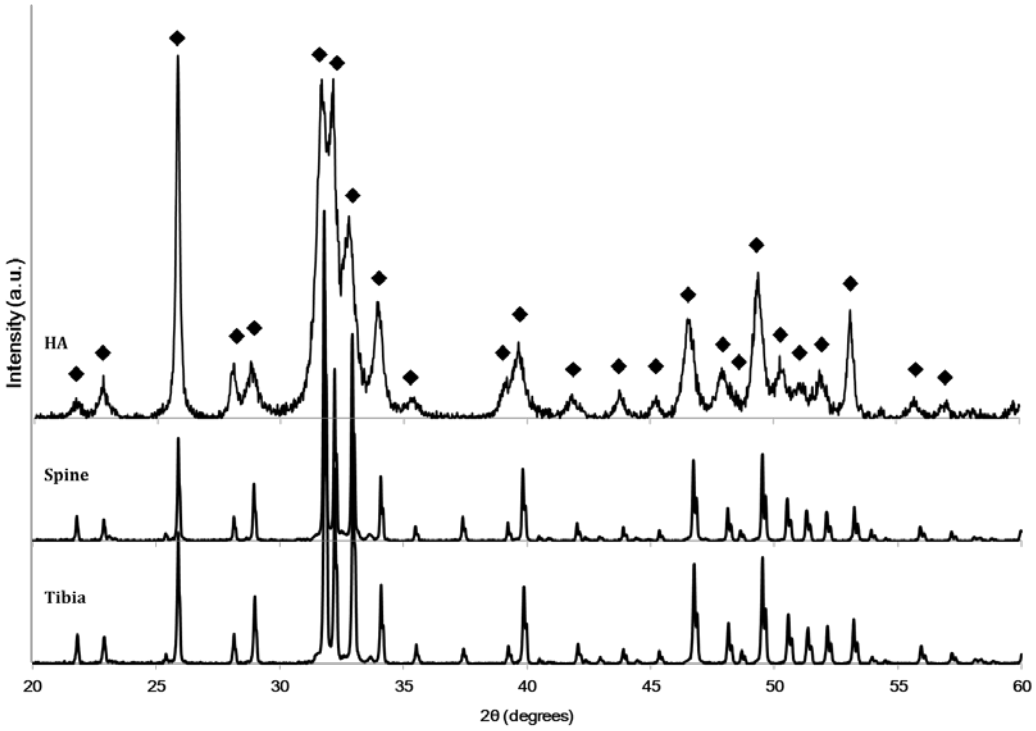

Fig. 5. XRD patterns according to the bone types and synthetic HA. (◆: Characteristic peaks of hydroxyapatite)

5.1.3 XRF

XRF analysis were carried out to figure out the chemical compositions. The chemical compositions of compact bone and cancellous bone were presented in Table Ⅲ. As seen, calcium, oxygen and phosphorous were the main components. And, some minor components such as sodium or magnesium were present. For the significance test, SAS 9.3 was used, and the significance was marked as *. There were significant differences only in Mg, Al, and K.

The chemical compositions of spine and tibia were presented in Table Ⅳ. They also

showed Ca, O, and P as major components and others as minor components. And in the significance test, there was no significant difference between spine and tibia. Although the Ca/P molar ratio was shown highly in spine, it was within the standard deviation.

Table III. Elemental composition according to the osseous tissue types.

Formula	Concentration (wt.%)			
	Compact bone		Cancellous bone	
		±S.D.		±S.D.
Ca	41.433	0.188	42.747	1.107
O	39.400	0.173	39.267	0.289
P	16.717	0.351	16.650	0.485
Na	1.096	0.164	0.491	0.387
Mg	0.567	0.019	0.521*	0.016
Al	0.297	0.072	0.000*	0.000
K	0.145	0.052	0.041*	0.002
Cl	0.122	0.022	0.077	0.031
S	0.116	0.022	0.102	0.021
Fe	0.063	0.024	0.043	0.015
Sr	0.058	0.002	0.064	0.004
Si	0.000	0.000	0.000	0.000
Ca/P molar ratio	1.916		1.984	

*, $p<0.05$

Table IV. Elemental composition according to the bone types.

Formula	Concentration (wt.%)			
	Spine		Tibia	
Ca	43.833	± 2.826	42.070	± 0.503
O	38.867	± 0.896	39.433	± 0.153
P	15.650	± 0.779	16.897	± 0.169
Na	0.335	± 0.163	0.571	± 0.082
Mg	0.460	± 0.060	0.528	± 0.033
Al	0.158	± 0.273	0.076	± 0.132
K	0.072	± 0.046	0.102	± 0.042
Cl	0.085	± 0.021	0.090	± 0.039
S	0.126	± 0.028	0.118	± 0.016
Fe	0.047	± 0.013	0.045	± 0.014
Sr	0.051	± 0.008	0.050	± 0.009
Si	0.319	± 0.553	0.000	± 0.000
Ca/P molar ratio	2.165		1.924	

In conclusion, although there were some non-detected bands, the presence of by-products, or the significant differences in some minor components, the differences were very small. So, it could be concluded that the type of osseous tissues and bone was not a considerable variable for the resultant horse bone powders.

5.2. Characteristics according to the pretreatment methods

5.2.1 FT-IR

Figure 6 showed the bands at 3640-3560 cm^{-1}, and 1088-962 cm^{-1}, which indicated OH and PO_4^{3-} group. No different bands were displayed according to the pretreatment methods. The hot water method and cold water method were expressed as HW and CW.

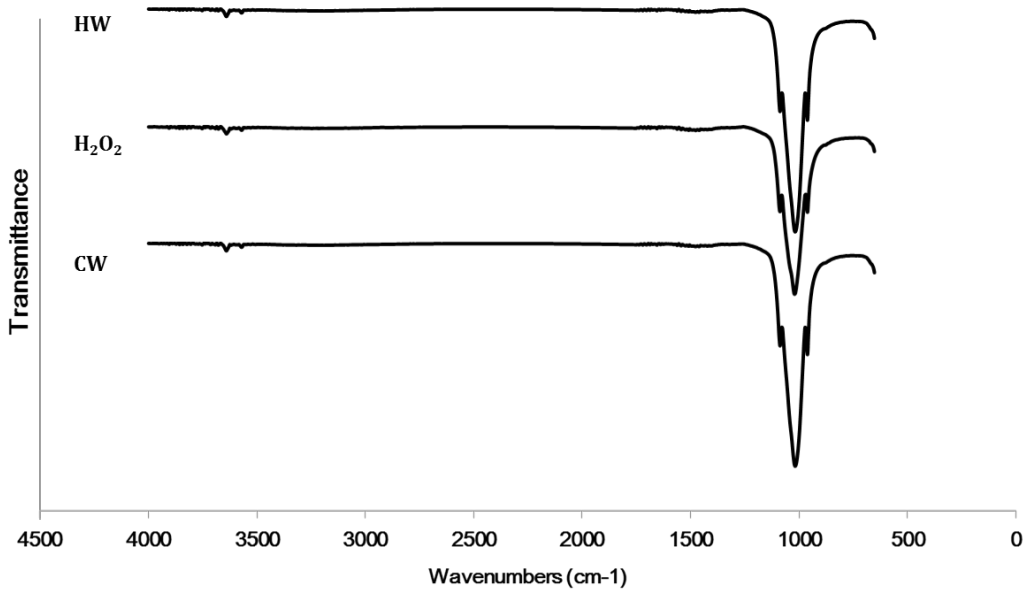

Fig. 6. FTIR spectra according to the pretreatment methods. (HW: hot water, CW: cold water)

5.2.2 XRD

Figure 7 showed the XRD patterns according to the pretreatment methods with the control group, synthetic HA. In the XRD patterns, the peaks were observed in same 2θ. The presence of CaO was also observed in all of the pretreatment methods.

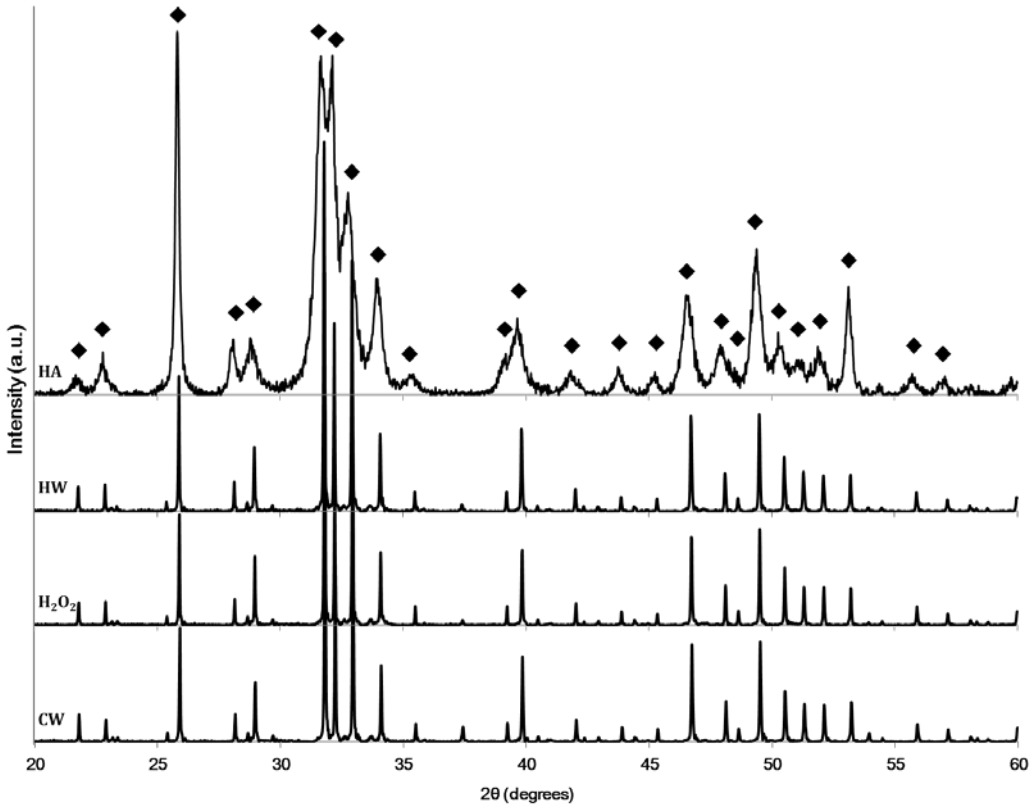

Fig. 7. . XRD patterns according to the pretreatment methods. (HW: hot water, CW: cold water, ◆: Characteristic peaks of hydroxyapatite)

5.2.3 XRF

The chemical compositions of compact bone and cancellous bone were presented in Table Ⅴ. It also showed the presence of calcium, oxygen and phosphorous as the main components with some minor components. The significant difference was displayed with *. The calcium was significantly low, and the phosphorous was significantly high in the hot water method. It was widely known that the ionic components of hydroxyapatite such

as Ca^{2+} can readily be exchanged by other ions [42]. Considering the significantly high contents of Na and K, it would be assumed that the Ca^{2+} components of hydroxyapatite were substituted by Na and K due to the relatively high temperature of hot water method.

In conclusion, there were no significant differences in FT-IR and XRD results according to the pretreatment methods, but there were some significant differences in element components. However, considering the differences were small, and the processing time in the hot water method was shorter (2 h) than the times of other pretreatment methods (48 h), the proper pretreatment method would be the hot water method.

Table V. Elemental composition according to the pretreatment methods. (HW: hot water, CW: cold water)

Formula	Concentration (wt.%)					
	CW		H_2O_2		HW	
Ca	44.023	± 0.107	44.047	± 0.085	*43.587	± 0.051
O	38.700	± 0.000	38.667	± 0.058	38.767	± 0.058
P	15.827	± 0.055	15.760	± 0.046	*15.967	± 0.035
Na	0.818	± 0.003	0.856	± 0.011	*0.978	± 0.018
Mg	*0.410	± 0.006	0.474	± 0.005	0.454	± 0.003
Al	0.020	± 0.006	0.009	± 0.016	0.018	± 0.016
K	0.037	± 0.002	0.038	± 0.001	*0.045	± 0.002
Cl	0.089	± 0.005	*0.042	± 0.003	0.084	± 0.002
S	0.048	± 0.001	0.054	± 0.001	*0.039	± 0.001
Fe	0.014	± 0.000	0.029	± 0.002	0.015	± 0.001
Sr	0.044	± 0.000	0.039	± 0.001	0.047	± 0.001
Zr	0.000	± 0.000	0.008	± 0.013	0.000	± 0.000
Ca/P molar ratio	2.150		2.160		2.110	

*, $p<0.05$

5.3. Sintering conditions

5.3.1. Sintering time selection

The sintering time was selected as enough time to eliminate the organic compounds, based on the several sintering steps with 4 h. The residual organic compounds were analyzed by FT-IR and the results were shown in Fig. 8. The broad band at 3448 cm^{-1} was shown in the spectrum of step 1 (4 h), which was assigned to the O-H stretch of water. The bands at 2205 cm^{-1} and 2106 cm^{-1} were assigned to the carbonyl stretch associated with the presence of aliphatic fatty acid. The broad and high bands at 1545 cm^{-1} and 1465 cm^{-1} were assigned to residual organic material although there would be a contribution from CO_3^{2-}. The bands under the 700 cm^{-1} were assigned to the CH groups in organic compounds [23].

In the spectrum of step 2 (8 h), there was no band related to the fatty acid and water, but weak bands at around 700 cm^{-1} due to the residual organic material.

Finally, in the spectrum of step 3 (12 h), all of the bands related to the organic compounds were absent. Consequently, sintering time would be 12 h to remove the residual organic compounds.

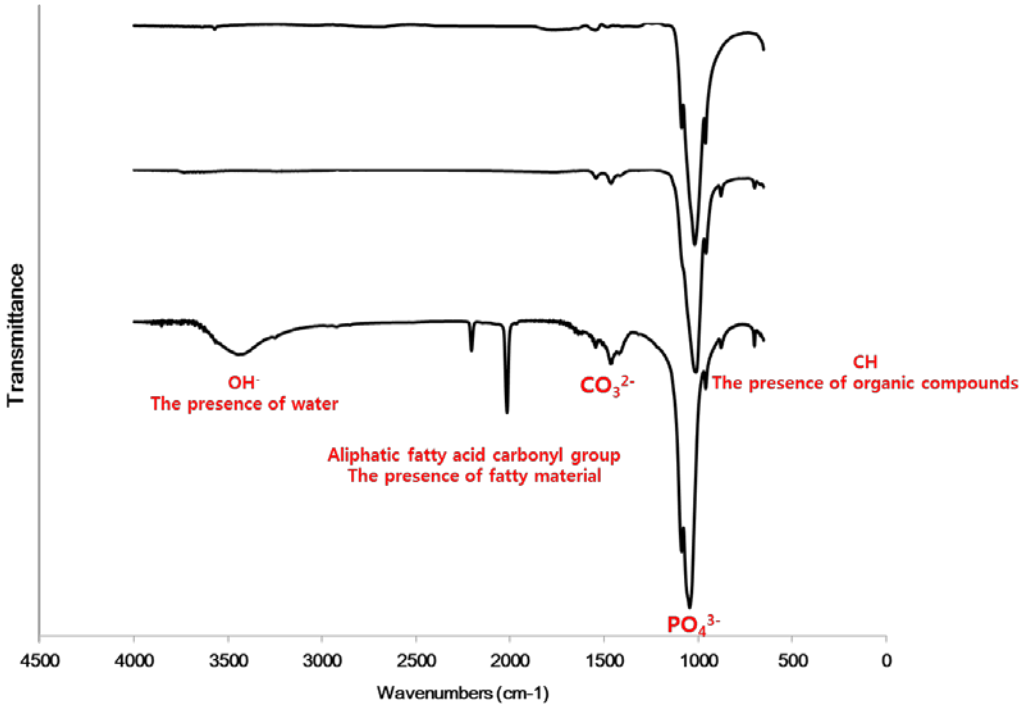

Fig. 8. FT-IR spectra according to the sintering time steps with 4 h.

5.3.2. Characteristics according to the sintering temperature

First, the sintering temperature was selected based on the TGA curve. The TGA curve was shown in Fig. 9. In the TGA results, the derivative weight had relationship with thermal changes. The thermal changes at 111.62℃ was related to the water evaporation (Fig. 9. A), and the thermal changes at 351.11℃ was related to the thermal reaction of organic compounds (Fig. 9. B). From the results, sintering at 600℃ could be enough to eliminate the organic compounds (Fig. 9. C). At 868.19℃, there was some thermal change would be assigned to the chemical decomposition (Fig. 9. D). And there was additional chemical decomposition at 1132.36℃ (Fig. 9. E). Therefore, 600℃, 900℃, 1100℃, and 1300℃

were selected as sintering temperature test groups. Specifically, TCP was observed in the sample sintered at 1300℃ (Fig. 9. F).

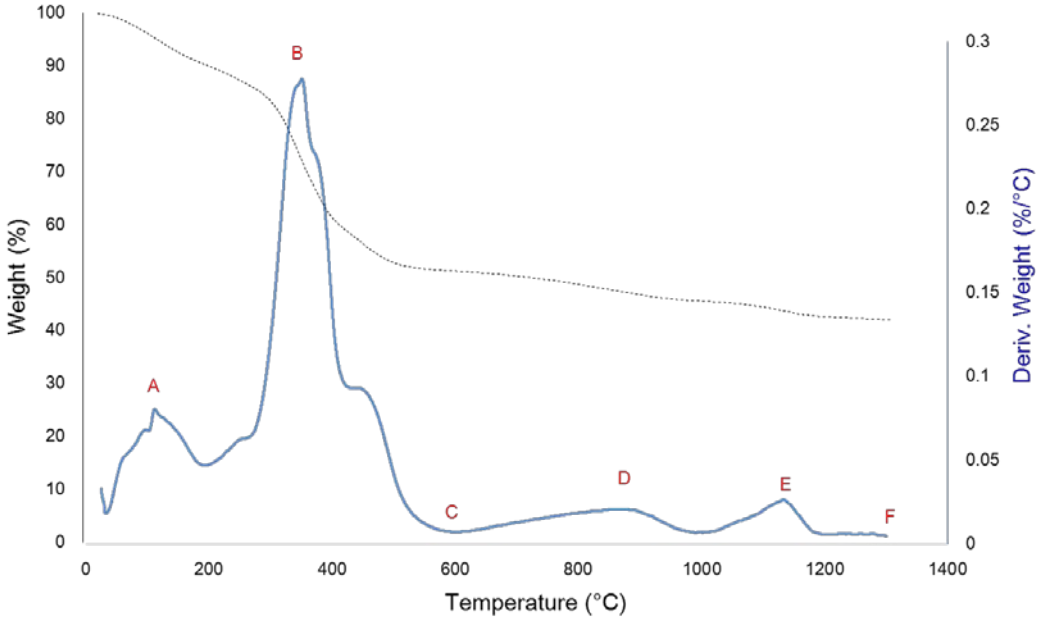

Fig. 9. TGA curve (black) and Derivative weight (blue) graph of horse bones.

A: Water evaporation, B: Thermal reaction of organic compounds, C: Elimination of organic compounds, D: Chemical decomposition, E: Additional chemical decomposition, F: TCP appearance

Figure 10 shows the FT-IR spectra of horse bone powders sintered at 600℃ (HB 600), 900℃ (HB 900), 1100℃ (HB 1100), and 1300℃ (HB 1300) with control groups (HA and Bio-Oss). Same bands with previous studies appeared at around 3570 cm^{-1}, 1455 cm^{-1}, 1416 cm^{-1}, 1088 cm^{-1}, 1017 cm^{-1}, 963 cm^{-1}, and 875 cm^{-1}. HA and HB 1300 showed absence of CO_3^{2-} bands. Bio-Oss, which was made from the bovine bone sintered at 600℃ showed

almost same bands with HB 600. In particular, the CO_3^{2-} bands were reduced according to the increase of sintering temperature. It could be attributed to the decomposition of carbonated calcium phosphate apatites ($Ca_{10}(PO_4)_6CO_3$) [43].

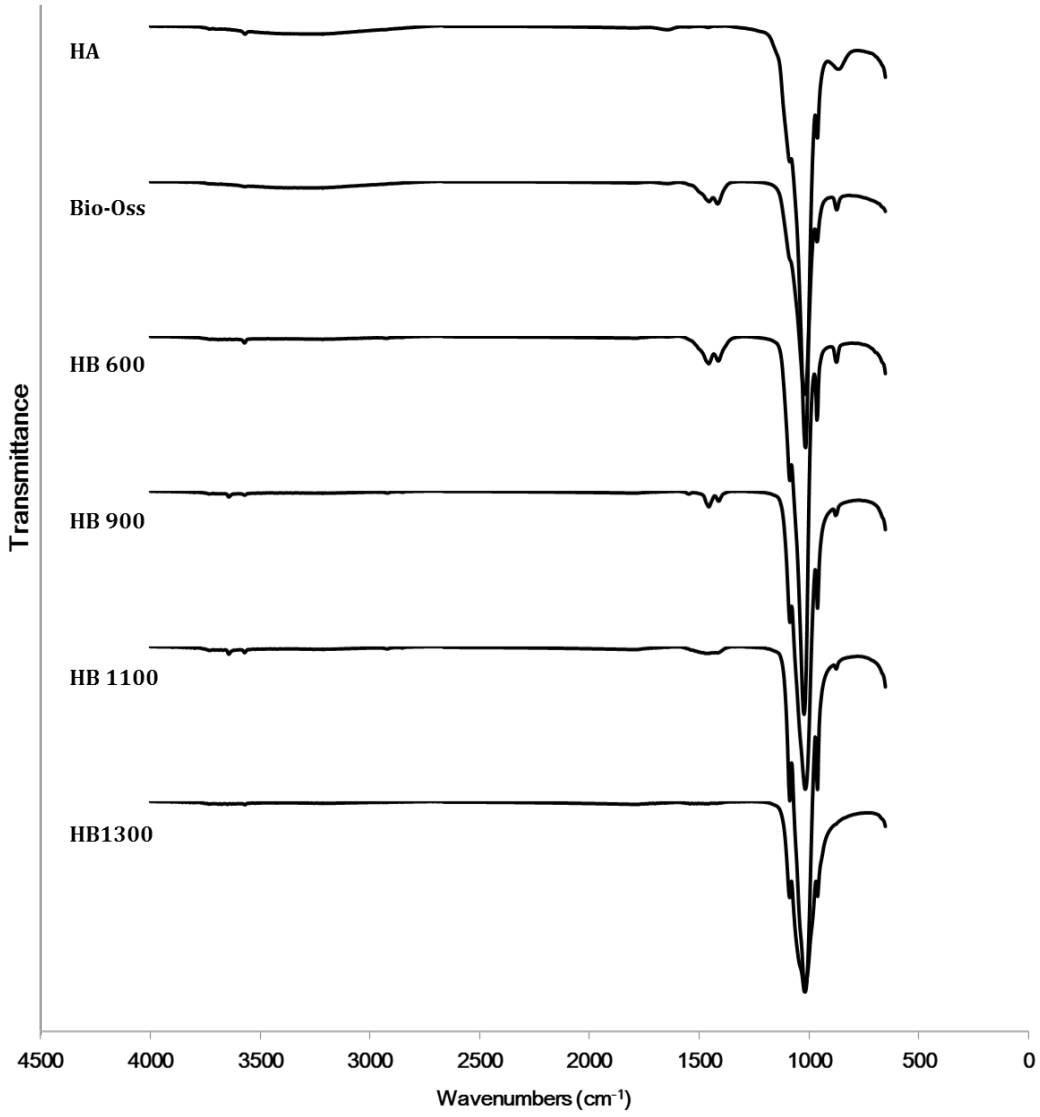

Fig. 10. FT-IR spectra of horse bone powders with different sintering temperature and control groups (HA and Bio-Oss).

Fig. 11 shows the XRD patterns of HB 600, HB 900, HB 1100, and HB 1300 with control groups (HA and Bio-Oss). The XRD patterns of HB 600 were completely corresponded to the XRD patterns of HA and Bio-Oss. The XRD patterns of HB 900 and HB 1100 showed the presence of CaO at 37° 2θ. However, the CaO peak was absent in HB 1300, Instead, the peak of calcium oxide phosphate appeared at 30° 2θ. It was reported that the reaction between the oxyhydroxyapatite and CaO occurred at around 1200℃ according to the following reaction [43]:

$$Ca_{10}(PO_4)_6(OH)_{2-2x}O_x \rightarrow 2Ca_3(PO_4)_2 + Ca_4O(PO_4)_2 + (1-x)H_2O$$

And the chemical compositions of the samples were presented in Table Ⅵ.

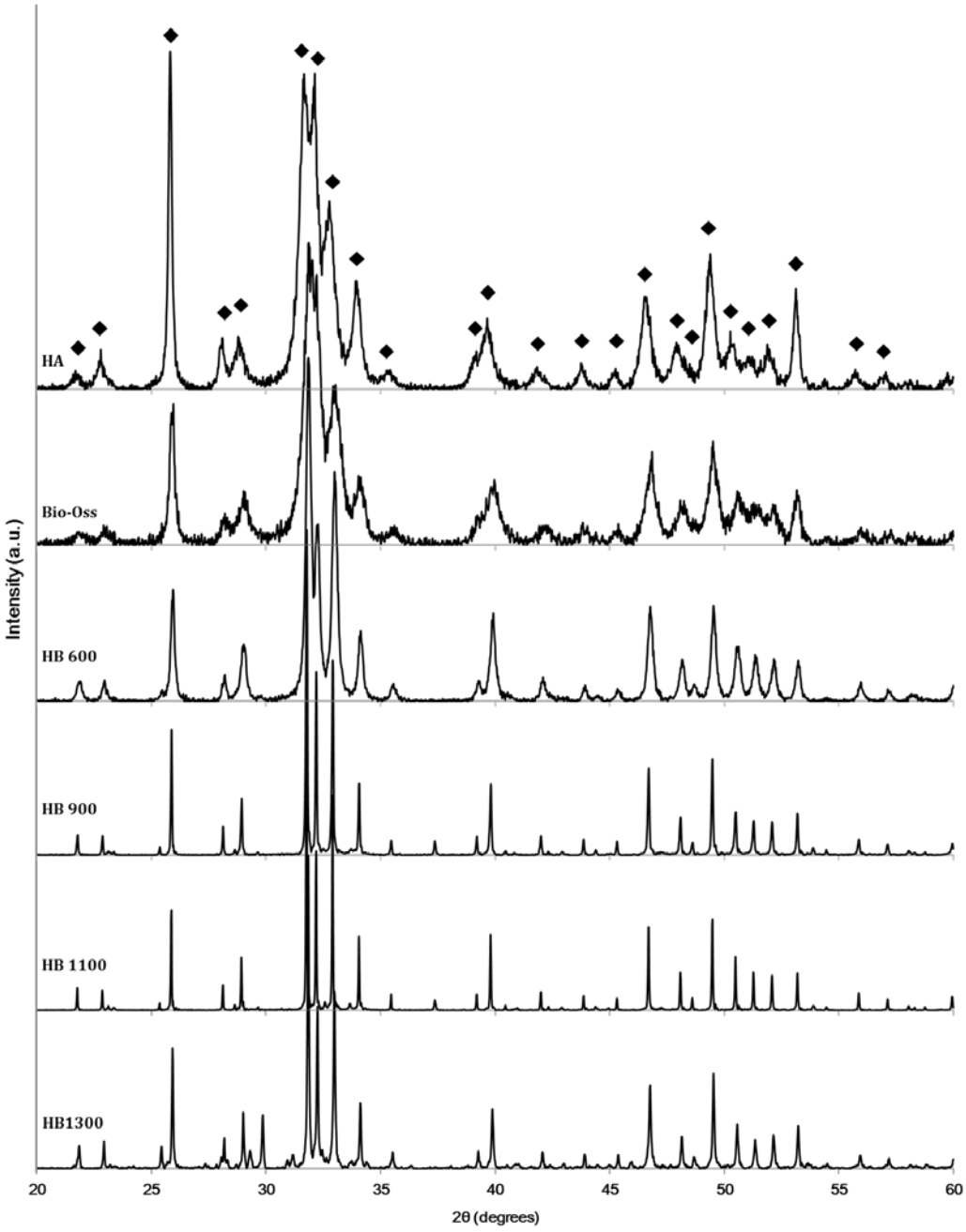

Fig. 11. XRD patterns according to the sintering temperature. (◆: Characteristic peaks of hydroxyapatite)

Table VI. Elemental composition according to the sintering temperature.

Formula	Concentration (wt.%)				
	HA	HB 600	HB 900	HB 1100	HB 1300
Ca	d38.050 ± 0.056	b42.227 ± 0.122	b42.193 ± 0.095	c41.567 ± 0.038	a42.993 ± 0.031
O	a40.700 ± 0.000	c39.367 ± 0.058	d39.267 ± 0.058	b39.567 ± 0.058	e39.100 ± 0.000
P	a19.267 ± 0.023	c16.910 ± 0.066	d16.787 ± 0.065	b17.217 ± 0.023	e16.510 ± 0.010
Na	a1.870 ± 0.017	d0.803 ± 0.008	b1.077 ± 0.012	c1.020 ± 0.010	d0.824 ± 0.009
Mg	d0.025 ± 0.001	a0.424 ± 0.001	b0.417 ± 0.004	a0.426 ± 0.002	d0.393 ± 0.006
Al	b0.000 ± 0.000	b0.000 ± 0.000	b0.000 ± 0.000	b0.000 ± 0.000	a0.016 ± 0.014
K	e0.000 ± 0.000	a0.044 ± 0.001	b0.039 ± 0.002	c0.031 ± 0.000	d0.026 ± 0.001
Cl	c0.035 ± 0.006	b0.093 ± 0.001	a0.145 ± 0.004	b0.093 ± 0.004	c0.031 ± 0.002
S	d0.000 ± 0.000	b0.046 ± 0.002	b0.045 ± 0.001	a0.049 ± 0.001	c0.040 ± 0.001
Fe	d0.000 ± 0.000	a0.015 ± 0.000	b0.012 ± 0.001	c0.010 ± 0.001	a0.014 ± 0.001
Sr	e0.010 ± 0.000	a0.063 ± 0.001	c0.034 ± 0.000	d0.033 ± 0.000	b0.036 ± 0.000
Zn	b0.000 ± 0.000	a0.016 ± 0.000	b0.000 ± 0.000	b0.000 ± 0.000	b0.000 ± 0.000
Ca/P molar ratio	1.526	1.930	1.943	1.866	2.013

- Means with the same letter are not significantly different.

The same letter means that there is no significant difference. Generally, the Ca/P molar ratio was higher in horse bone samples than in HA. And the Ca/P ratio increased according to the increase of the sintering temperature, except the HB 1100. It would be attributed to the CaO. It was reported that the CaO contents increased with the increasing sintering temperature [44].

The FE-SEM images of samples were shown in Fig. 12. The horse bone powders were merged due to the changes under sintering [45]. The surface of HA and Bio-Oss consisted of nano scale blocks, which may be the influence of chemical treatment during their production.

In summary, the sintering temperature influenced strongly to the resultant horse bone powders. In particular, Ca/P molar ratio increased according to the increase of the sintering temperature due to the increasing CaO. However, horse bone powders sintered at 1100℃ was not matched with the tendency. The reason would be unknown.

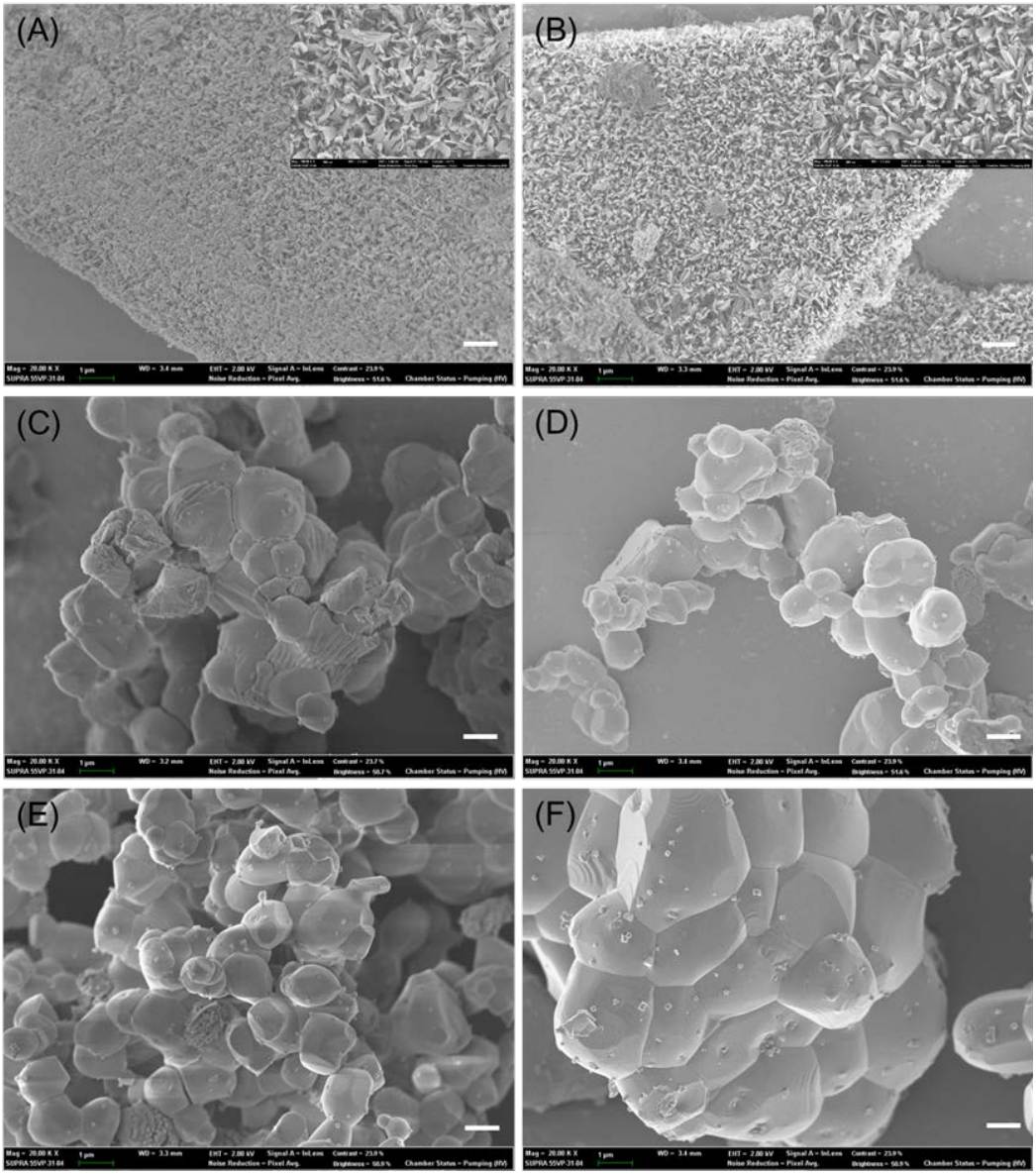

Fig. 12. SEM images of horse bone powders and control groups (HA and Bio-Oss). The control groups are displayed with the magnified images; (A) HA, (B) Bio-Oss, (C) HB 600, (D) HB 900, (E) HB 1100, and (F) HB 1300. Scale bar = 1 μm.

5.4. Grinding methods

For the powder size analysis, the Malvern Mastersizer S was used, and the results were shown in Fig. 13. The average size of particles from the ball mill method was 2.888 μm, and the average size of particles from the blade grinder method was 4.527 μm. However, the distribution of particles from blade grinder was closer to the normal distribution. Considering it, the grinding quality of resultant powders would be better in blade grinder method. The work efficiency was also higher in blade grinder method (2 kg/hour) than in ball mill method (50 g/hour). Furthermore, SEM images of the powders from the blade grinder method showed the powders were aggregated due to the properties of nano size particles (Fig. 14). As described, it was reported that the nano size hydroxyapatite showed better cell proliferation and inhibition of cell apoptosis [37, 38]. Although the particles were not dispersed, the blade grinder method showed enough potential to produce nano size powders.

In summary, the particle distribution quality and work efficiency were better in the blade grinder method and although the average size from the blade grinder method was larger, the difference was low and the main problem of the size was aggregation of the particles. So, we can conclude that the blade grinder method would be better than the ball mill method.

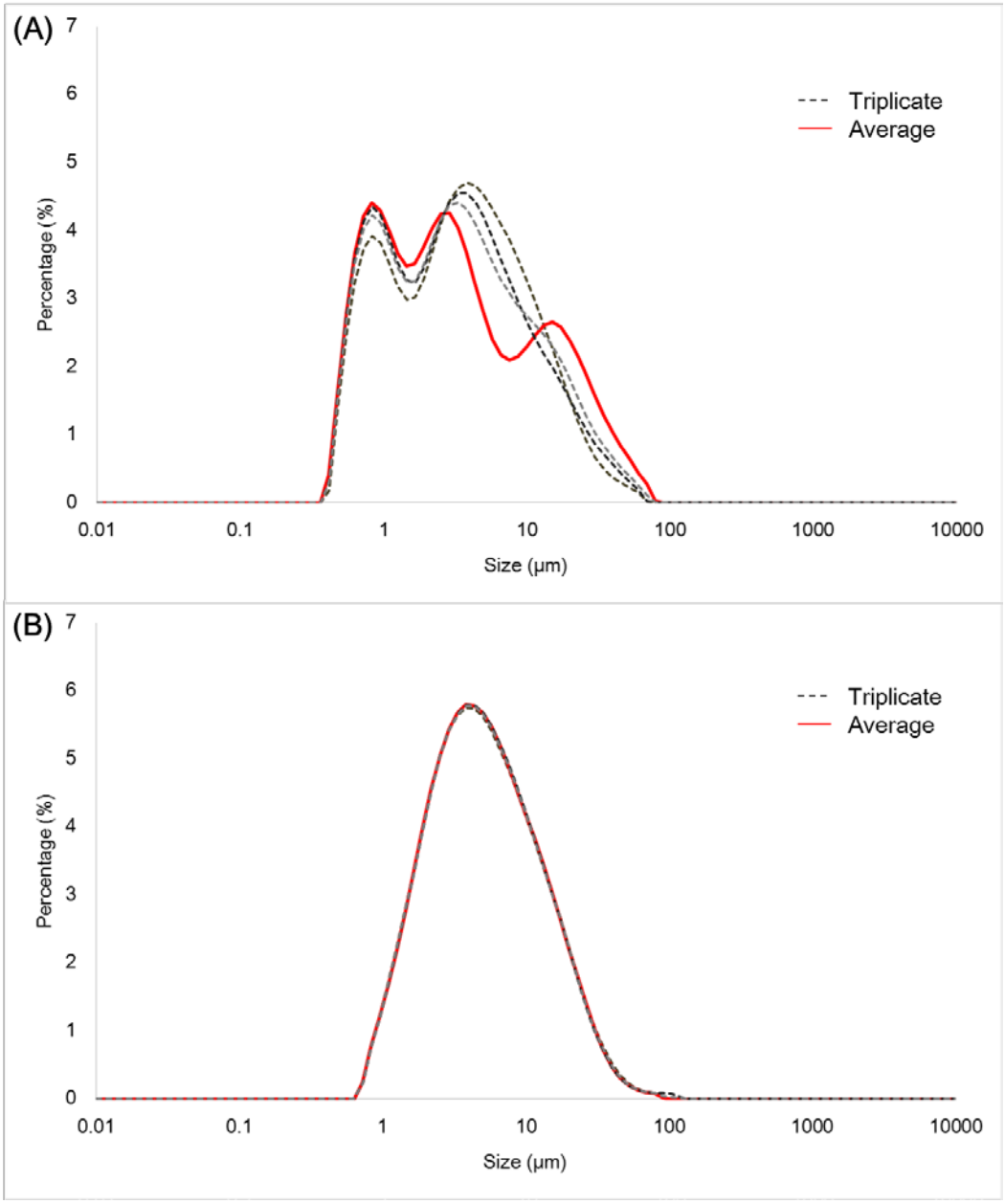

Fig. 13. The particle distribution of (A) ball mill (wet grinding) and (B) blade grinder (dry grinding).

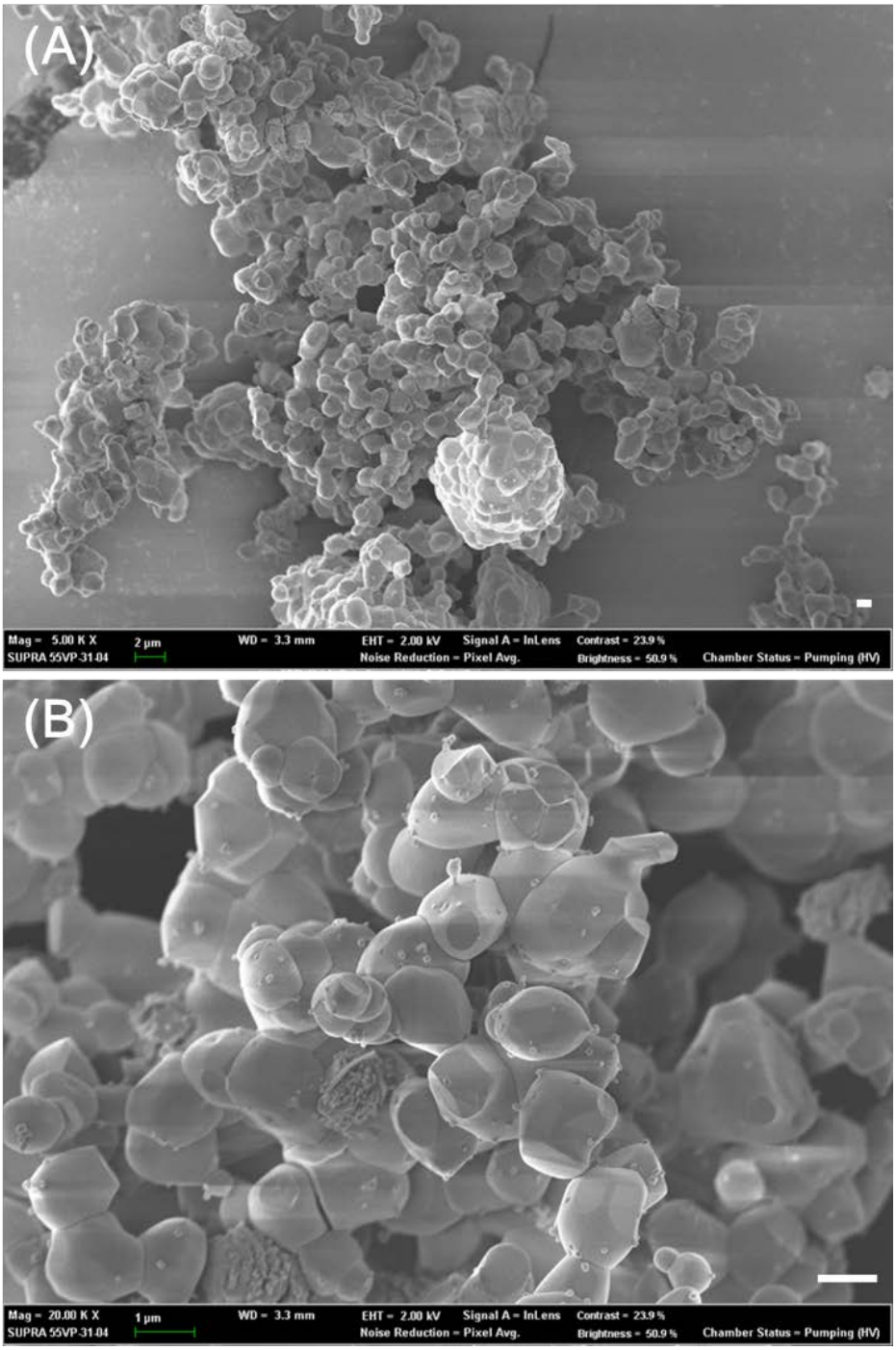

Fig. 14. SEM images of the powders from blade grinder method with (A) x5000 magnification and (B) x20000 magnification.

5.5. *In vitro* test

5.5.1. Cell toxicity test

The results of the WST cytotoxicity assay using MC3T3-E1 osteoblast-like cells are arranged by samples (Fig. 15) and time (hour) (Fig. 16). The significant difference was marked with * and letters. The same letters mean that there is no significant difference. Figure 15 shows there was significant cell proliferation according to the times, which mean cells grew well.

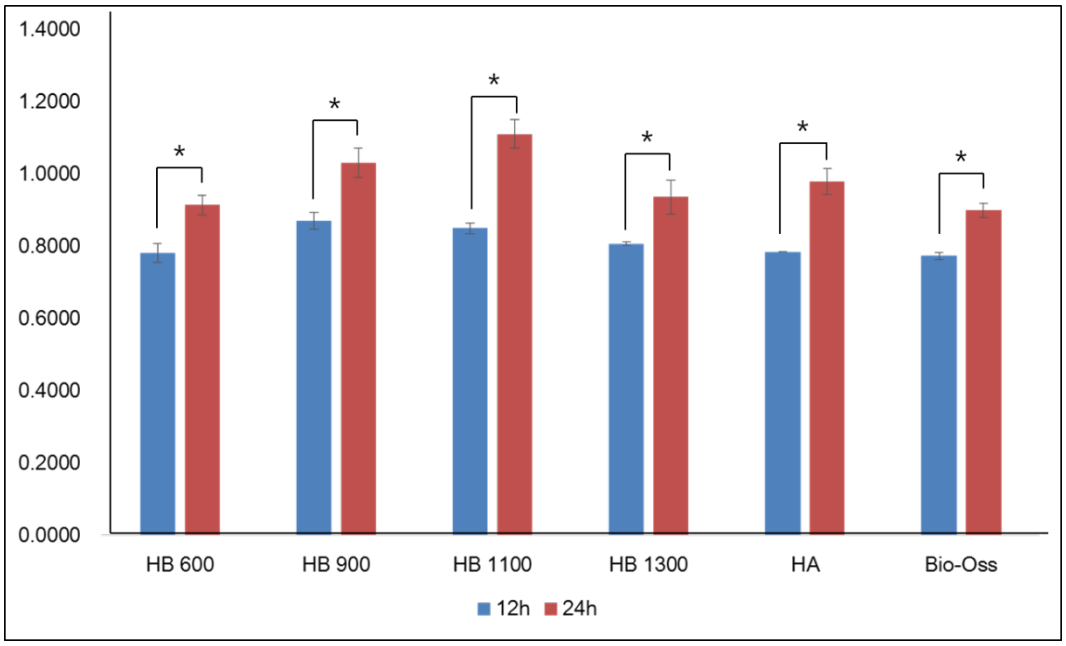

Fig. 15. Cell viability arranged by the samples with different sintering temperature samples and control groups (HA and Bio-Oss). *, $p<0.05$. Error bars represent standard deviation, n=3.

Figure 16 shows the cell viability was higher in HB 900 and HB 1100 after 12 h, but after 24 h, HB 1100 showed the highest cell viability. The control groups showed almost same

cell viability with HB 600 and HB 1300. It would be assumed that the CaO might influence the cell toxicity. HB 900 and HB 1100 had higher CaO contents than HB 600 and HB 1300, and they showed better cell viability. However, the CaO contents were at most 7% according to the XRD analysis (not shown), so it was not certain that the small contents would be the main factor for these results.

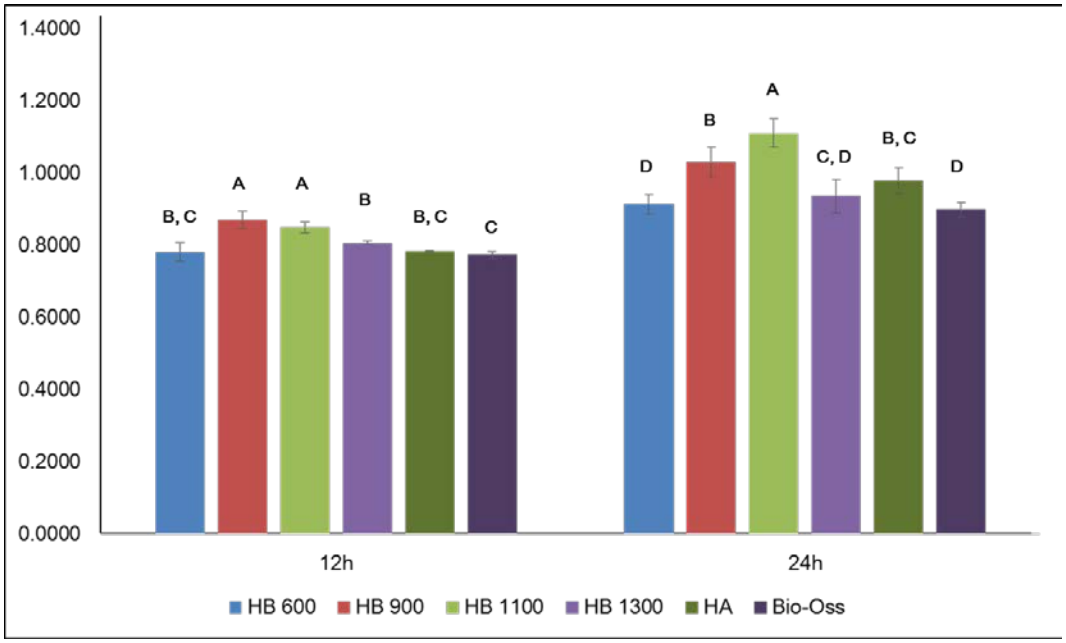

Fig. 16. Cell viability on the horse bone powders sintered at the different temperature, arranged by the times (hours) with different sintering temperature samples and control groups (HA and Bio-Oss). Means with the same letter are not significantly different. Error bars represent standard deviation, n=3.

5.5.2. Cell proliferation test

For more long period observation of cell viability, cell proliferation test was conducted, and the results were arranged by samples (Fig. 17) and time (day) (Fig. 18). In contrast with the cell toxicity test, Figure 17 shows that cell viability of samples decreased according to the days. The control groups maintained almost same cell viability or showed the increased cell viability.

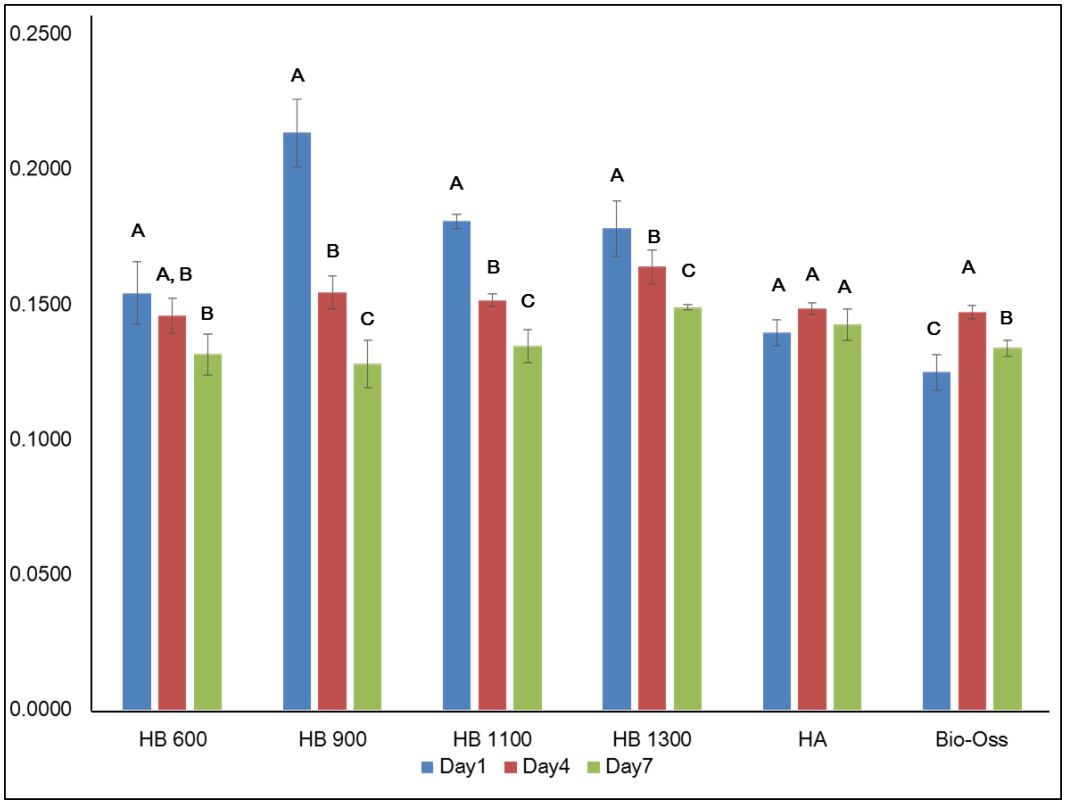

Fig. 17. Cell proliferation on the horse bone powders sintered at the different temperature, arranged by samples with different sintering temperature samples and control groups (HA and Bio-Oss). Means with the same letter are not significantly different. Error bars represent standard deviation, n=3.

In Fig 18, HB 900 showed the most promoted cell viability in 1 day, but in 4 and 7 days, cell viability of HB 1300 showed the most promoted cell viability. In particular, the sintered horse bone powders showed better cell viability in 1 day, and HB 1100 and HB 1300 maintained the similar or better cell viability in 4 days and 7 days. The decrease on cell viability of samples would be due to the non-treated surface or PDMS. Indeed, the cells on unmodified PDMS surface could restrain the cell proliferation in our study (not shown). As seen in Fig. 12, HA and Bio-Oss had chemically treated surface, and it would contribute to the promoted cell proliferation. However, HB 1100 and 1300 showed similar or better cell viability with the control groups. And it suggested that these developed horse bone powders have enough potential as a biomaterial.

The reason of promoted cell proliferation on the horse bone powders sintered at high temperature could be found in the previous studies. Laquerriere et al. (2001) and Wang et al. reported that the hydroxyapatite sintered at higher temperature showed more promoted cell proliferation and lower cell toxicity [46, 47]. They assumed the results would be caused by the crystal size and dissolution rate. They reported that the higher sintering temperature enhanced the crystal particle growth and showed a lower dissolution rate. And, the dissolution of the particles leads to the release of calcium ions or phosphorous ions and there is a decrease of the pH close to the hydroxyapatite causing partial dissolution of the crystal, an increase in the concentration of calcium and phosphate ions (the majority component of the crystal), and the formation of CO_3^-apatite crystals from the biological fluids. Then these ions could interact with channels and concentrations of diffusible ions, and finally cause the membrane depolarization, which could induce activation of

transcription factors in the cell nucleus and gene expression [46].

Our result was in agreement with their reports. Specifically, the crystal sizes of the powders according to the sintering temperature were analyzed by TOPAS software (Table Ⅶ). Specifically, the crystal size increased along the sintering temperature, but the crystal size rather decreased in 1300℃. Considering the elemental compositions, it would be influenced by CaO decomposition in 1300℃. As described, HB 1300 would be with $Ca_3(PO_4)_2$ and $Ca_4O(PO_4)_2$, which have lower dissolution rate than CaO. In addition there would be a small quantity of $Ca_3(PO_4)_2$ or $Ca_4O(PO_4)_2$ in HB 1300, there was HA/TCP composite surface and it would be another factor for the promoted cell proliferation in HB 1300. Indeed, Tanimoto et al. reported the promotion of cell proliferation in HA/TCP composite ceramics, but the mechanism was not disclosed [48]. And, although HB 600 had no CaO, it had very small crystal particle size. Therefore, it had high specific area and would have high dissolution rate.

Based on the above results, although initial cell adhesion would be better using HB 900 or HB 1100, HB 1300 would be the most suitable for more long time cell proliferation.

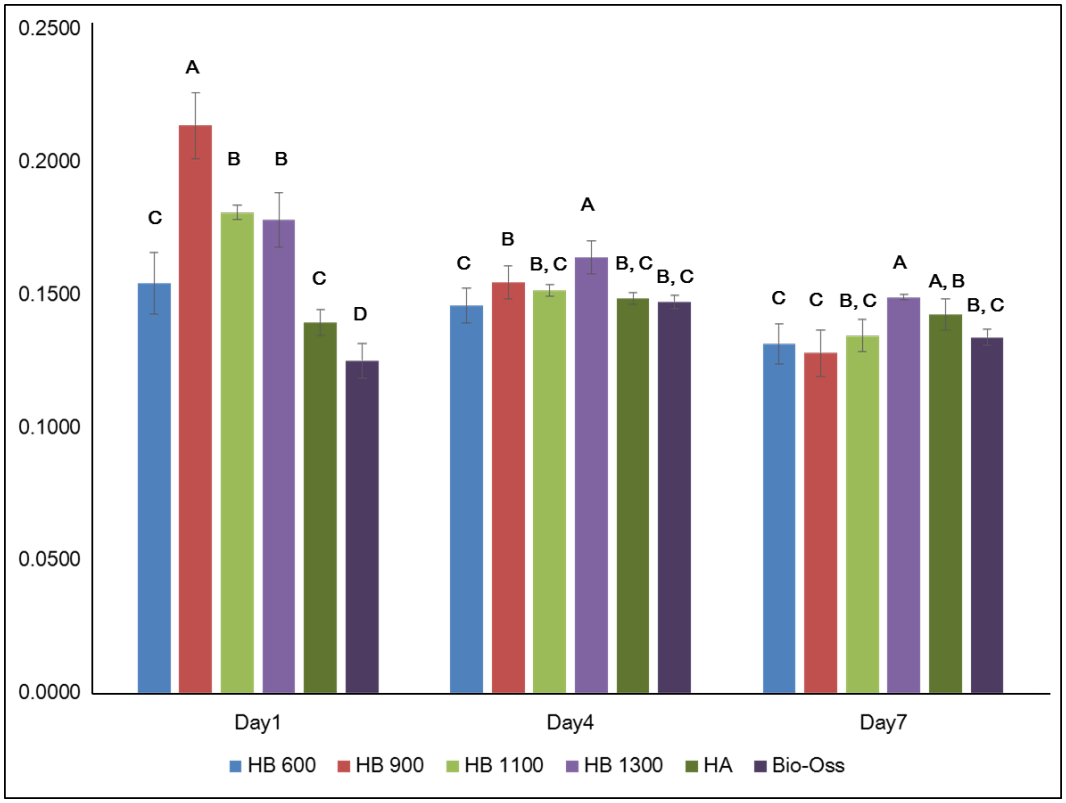

Fig. 18. Cell proliferation on the horse bone powders sintered at the different temperature, arranged by days with different sintering temperature samples and control groups (HA and Bio-Oss). Means with the same letter are not significantly different. Error bars represent standard deviation, n=3.

Table VII. The crystalline sizes of the powders according to the sintering temperature.

Sample	HB 600	HB 900	HB 1100	HB 1300	HA	Bio-Oss
Crystal size (nm)	50.5	288	556	116.7	22.86	17.64

6. Conclusions

The objectives of this study were to develop and evaluate new develop new calcium phosphate using sintered horse bones and to optimize the method for the production of the natural calcium phosphate derived from horse bones. In this study, the followings are the main results:

1) The characteristics according to the types of osseous tissue and bone were investigated. There was no significant difference in FT-IR spectra and XRD patterns according to the types of osseous tissue and bone. And there was no significant difference in major components of XRF results. It suggests that the type of osseous tissues and bone is not a considerable factor in resultant bone powders, so the selection or separation process could be skipped.

2) The characteristics according to the pretreatment methods were investigated. There was no significant difference in FT-IR spectra and XRD patterns according to the pretreatment methods. And although hot water showed low Ca/P ratio, the difference was very small and the processing time (2 h) was shorter than others (48 h). Considering it, hot water method would be the most efficient preparation method.

3) The sintering time which was enough to eliminate the residual organic compounds was selected based on the FT-IR spectra of the stepwise sintering process. There were FT-IR

bands in step 1 (4 h) and step 2 (8 h), which indicated the presence of the residual organic compounds, but they disappeared at step 3 (12 h). It showed the sintering process for 12 h was enough.

4) The characteristics according to the sintering temperature were investigated. The sintering temperature, 600℃, 900℃, 1100℃, and 1300℃ were selected based on the TGA curve, considering the thermal change peaks. In FT-IR, the bands for CO_3^{2-} were reduced according to the increase of the sintering temperature, which indicated the decomposition was occurred. And XRD results showed the presence of CaO at 900℃ and 1100℃, but the CaO was decomposed to tri-calcium phosphate and calcium oxide phosphate at 1300℃. XRF results showed the increase of the Ca/P molar ratio according to the increase of the sintering temperature, except HB 1100. In SEM images, synthetic hydroxyapatite and Bio-Oss showed the specific surface made by chemical treatment, while sintered horse bone powders showed the merged particles due to the sintering process.

5) Two types of grinding method (ball milling and blade grinder) were tested. The ball milling method showed smaller average particle size, but the distribution quality and work efficiency were higher in the blade grinder method. In additional SEM images, the nano powders were aggregated into micro size. So, the micro average size was not important, but the dispersant for the nano size particles would be important. For these reasons, the blade grinder method would be better grinding method.

6) In vitro test was carried out using the horse bone powders from different temperature and control groups (synthetic hydroxyapatite and Bio-Oss). In cell toxicity test, HB 1100 showed the highest cell viability. On the contrary, HB 900 showed the highest cell viability in 1 day, and HB 1300 showed the highest cell viability in 4 and 7 days on cell proliferation test. Based on these results, for the initial cell adhesion, it would be better using HB 900 or HB 1100, but for more long time cell proliferation, HB 1300 would be the most suitable.

Finally, the optimized horse bone powder production process was constructed and it would be 1) horse bone preparation with cutting the flesh, 2) washing with distilled water for 48 h, 3) hot water pretreatment for 2 h, 4) cleaning with distilled water one more and drying, 5) sintering for 12 h at 1300℃, 6) grinding with blade grinder (Fig. 18). And, it was demonstrated that this horse bone powder had a great potential as biomaterials for bone tissue engineering.

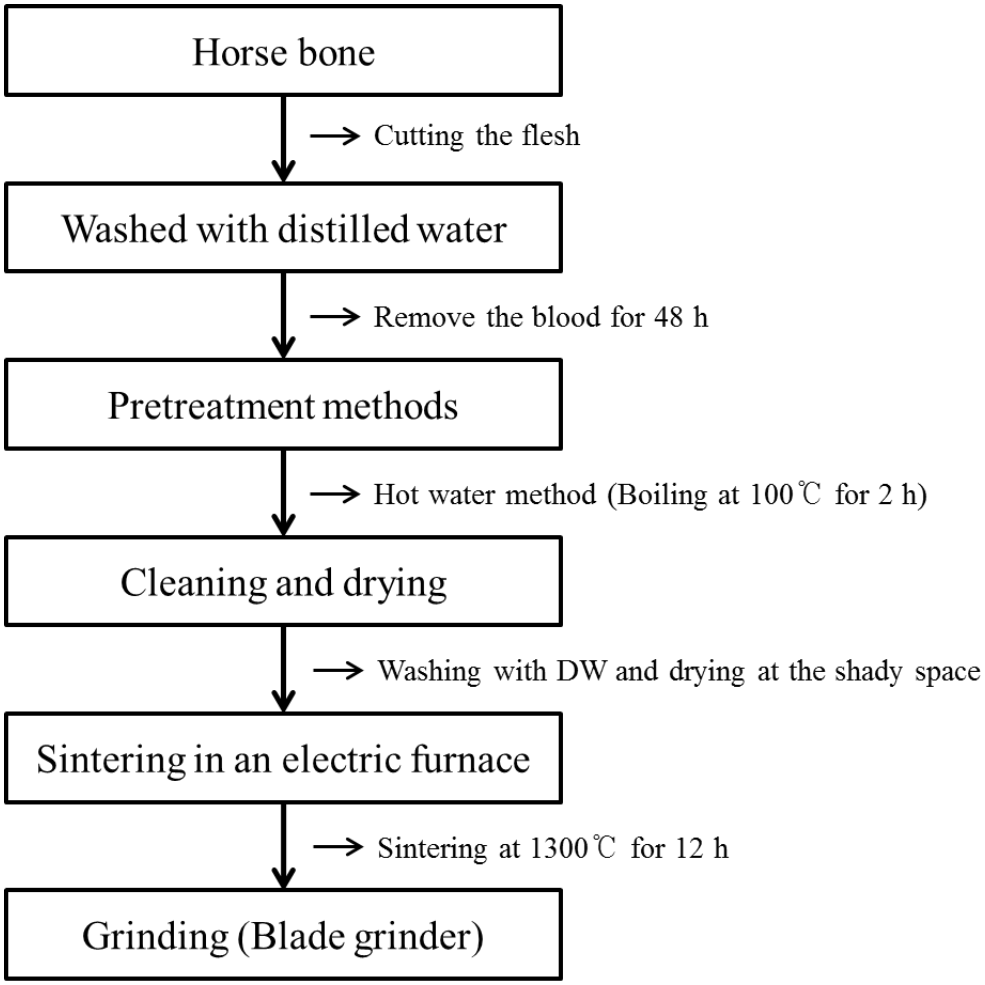

Fig. 19. The schematic design of the optimized horse bone powder production process

7. References

1. Langer, R. and J.P. Vacanti, *Tissue engineering*. Science, 1993. **260**(5110): p. 920-6.
2. Skalak, R. and C. Fox, *Tissue Engineering, Alan R. Liss.* Inc., New York, 1988.
3. Hench, L.L., *Biomaterials: a forecast for the future.* Biomaterials, 1998. **19**(16): p. 1419-23.
4. Johnell, O. and J.A. Kanis, *An estimate of the worldwide prevalence and disability associated with osteoporotic fractures.* Osteoporos Int, 2006. **17**(12): p. 1726-33.
5. Betz, R.R., *Limitations of autograft and allograft: new synthetic solutions.* Orthopedics, 2002. **25**(5 Suppl): p. s561-70.
6. Moore, W.R., S.E. Graves, and G.I. Bain, *Synthetic bone graft substitutes.* ANZ J Surg, 2001. **71**(6): p. 354-61.
7. Ueno, Y., et al., *Studies of sintered bone as a bone substitute.* Orthop Ceramic Implants, 1983. **3**: p. 11-16.
8. Taniguchi, Y., et al., *Sintered bone implantation for the treatment of benign bone tumours in the hand.* J Hand Surg Br, 1999. **24**(1): p. 109-12.
9. Sobczak, A., Z. Kowalski, and Z. Wzorek, *Preparation of hydroxyapatite from animal bones.* Acta Bioeng Biomech, 2009. **11**(4): p. 23-8.
10. Guizzardi, S., et al., *Qualitative assessment of natural apatite in vitro and in vivo.* J Biomed Mater Res, 2000. **53**(3): p. 227-34.
11. Mezahi, F.Z., et al., *Dissolution kinetic and structural behaviour of natural hydroxyapatite vs. thermal treatment.* Journal of Thermal Analysis and Calorimetry, 2009. **95**(1): p. 21-29.
12. Im, A., et al., *Preparation and biocompatibility of composite bone scaffolds using gnotobiotic pig bones.* Journal of Biosystems Engineering, 2007. **32**.
13. Janus, A.M., et al., *Chemical and microstructural characterization of natural hydroxyapatite derived from pig bones.* Microchimica Acta, 2008. **161**(3-4): p. 349-353.
14. Tsai, W.C., et al., *Clinical result of sintered bovine hydroxyapatite bone substitute: analysis of the interface reaction between tissue and bone substitute.* Journal of Orthopaedic Science, 2010. **15**(2): p. 223-232.
15. Barakat, N.A.M., et al., *Physiochemical characterizations of hydroxyapatite extracted from bovine bones by three different methods: Extraction of biologically desirable HAp.* Materials Science & Engineering C-Biomimetic and Supramolecular Systems, 2008. **28**(8): p. 1381-1387.
16. Kim, H., C. Rey, and M.J. Glimcher, *X-ray diffraction, electron microscopy, and Fourier transform infrared spectroscopy of apatite crystals isolated from chicken and bovine calcified cartilage.* Calcif Tissue Int, 1996. **59**(1): p. 58-63.
17. Ozawa, M. and S. Suzuki, *Microstructural Development of Natural Hydroxyapatite Originated from Fish-Bone Waste through Heat Treatment.* Journal of the American Ceramic Society, 2002. **85**(5): p. 1315-1317.
18. Mondal, S., et al., *Studies on Processing and Characterization of Hydroxyapatite Biomaterials from Different Bio Wastes.* Journal of Minerals & Materials Characterization, 2012: p. 55-67.
19. 김용준, et al., *말도체 연령 추정을 위한 사육 개월령별 말도체흉추골의 골화상태 비교.* 현장연구조사 목적 및 범위, 2012: p. 113.
20. Panda, N.N., K. Pramanik, and L.B. Sukla, *Extraction and characterization of*

biocompatible hydroxyapatite from fresh water fish scales for tissue engineering scaffold. Bioprocess Biosyst Eng, 2013: p. 1-8.
21. Fernandez-Moran, H. and A. Engstrom, *Electron microscopy and x-ray diffraction of bone.* Biochim Biophys Acta, 1957. **23**(2): p. 260-4.
22. Wang, X.-Y., et al., *Comparative study on inorganic composition and crystallographic properties of cortical and cancellous bone.* Biomedical and Environmental Sciences, 2010. **23**(6): p. 473-480.
23. Laird, D.F., *Reinforced Sintered Cancellous Bovine Bone as a Potential Bone Replacement Material*, 2010, University of Waikato.
24. Ooi, C.Y., M. Hamdi, and S. Ramesh, *Properties of hydroxyapatite produced by annealing of bovine bone.* Ceramics International, 2007. **33**(7): p. 1171-1177.
25. Danilchenko, S., et al., *Thermal behavior of biogenic apatite crystals in bone: An X-ray diffraction study.* Crystal Research and Technology, 2006. **41**(3): p. 268-275.
26. Baik, S.J., *Development of Fast-Hardening Calcium Phosphate Cement Using Sintered Animal Bone Powders and Chitosan Solution for Bone Tissue Engineering*, 2011, Seoul National University: Seoul.
27. Quarles, L.D., et al., *Distinct proliferative and differentiated stages of murine MC3T3-E1 cells in culture: An in vitro model of osteoblast development.* Journal of Bone and Mineral Research, 1992. **7**(6): p. 683-692.
28. Wang, J., J. de Boer, and K. de Groot, *Proliferation and differentiation of MC3T3-E1 cells on calcium phosphate/chitosan coatings.* J Dent Res, 2008. **87**(7): p. 650-4.
29. Albee, F.H., *Studies in bone growth: triple calcium phosphate as a stimulus to osteogenesis.* Annals of surgery, 1920. **71**(1): p. 32.
30. Ray, R. and A. Ward Jr. *A preliminary report on studies of basic calcium phosphate in bone replacement*. in *Surgical forum*. 1951.
31. Monroe, E.A., et al., *New calcium phosphate ceramic material for bone and tooth implants.* J Dent Res, 1971. **50**(4): p. 860-1.
32. Getter, L., et al., *Three biodegradable calcium phosphate slurry implants in bone.* J Oral Surg, 1972. **30**(4): p. 263-8.
33. Jarcho, M., et al., *Hydroxylapatite Synthesis and Characterization in Dense Polycrystalline Form.* Journal of Materials Science, 1976. **11**(11): p. 2027-2035.
34. de Groot, K., *Bioceramics consisting of calcium phosphate salts.* Biomaterials, 1980. **1**(1): p. 47-50.
35. Matsumoto, T., et al., *Effects of sintered bovine bone on cell proliferation, collagen synthesis, and osteoblastic expression in MC3T3-E1 osteoblast-like cells.* Journal of orthopaedic research, 1999. **17**(4): p. 586-592.
36. Liu, Q., et al., *Insight into Biological Apatite: Physiochemical Properties and Preparation Approaches.* BioMed research international, 2013. **2013**.
37. Cai, Y.R., et al., *Role of hydroxyapatite nanoparticle size in bone cell proliferation.* Journal of Materials Chemistry, 2007. **17**(36): p. 3780-3787.
38. Shi, Z., et al., *Size effect of hydroxyapatite nanoparticles on proliferation and apoptosis of osteoblast-like cells.* Acta Biomater, 2009. **5**(1): p. 338-45.
39. Yuan, Y., et al., *Size-mediated cytotoxicity and apoptosis of hydroxyapatite nanoparticles in human hepatoma HepG2 cells.* Biomaterials, 2010. **31**(4): p. 730-40.
40. Zhou, H. and J. Lee, *Nanoscale hydroxyapatite particles for bone tissue engineering.* Acta Biomater, 2011. **7**(7): p. 2769-81.
41. Rodrigues, C., et al., *Characterization of a bovine collagen–hydroxyapatite composite scaffold for bone tissue engineering.* Biomaterials, 2003. **24**(27): p. 4987-4997.

42. Bahrololoom, M.E., et al., *Characterisation of natural hydroxyapatite extracted from bovine cortical bone ash.* Journal of Ceramic Processing Research, 2009. **10**(2): p. 129-138.
43. Lafon, J.-P., et al., *Termal decomposition of carbonated calcium phosphate apatites.* Journal of thermal analysis and calorimetry, 2003. **72**(3): p. 1127-1134.
44. Haberko, K., et al., *Natural hydroxyapatite—its behaviour during heat treatment.* Journal of the European Ceramic Society, 2006. **26**(4): p. 537-542.
45. Dorozhkin, S.V., *Calcium orthophosphates as bioceramics: state of the art.* Journal of Functional Biomaterials, 2010. **1**(1): p. 22-107.
46. Laquerriere, P., et al., *Effect of hydroxyapatite sintering temperature on intracellular ionic concentrations of monocytes: A TEM-cryo-x-ray microanalysis study.* Journal of biomedical materials research, 2001. **58**(3): p. 238-246.
47. Wang, C.Y., et al., *Proliferation and bone-related gene expression of osteoblasts grown on hydroxyapatite ceramics sintered at different temperature.* Biomaterials, 2004. **25**(15): p. 2949-2956.
48. Tanimoto, Y., et al., *Effect of Varying HAP/TCP Ratios in Tape-cast Biphasic Calcium Phosphate Ceramics on Response in vitro.* Journal of Hard Tissue Biology, 2009. **18**(2): p. 71-76.

말 뼈를 이용한 천연 인산칼슘계 생체소재 개발

서울대학교 대학원

바이오시스템·소재학부 바이오시스템공학전공

조 우 재

초 록

인산 칼슘은 뼈와 치아 등의 인체 경조직의 주요 성분이다. 이 때문에, 인산 칼슘은 의료분야 (예를 들면 치과용 충전제, 골 지지체, 그리고 골 시멘트 등)에 적용하기 위해 연구되어 왔다. 특히, 인산 칼슘의 한 종류인 수산화인회석 (HA, Ca10(PO4)6(OH)2)은 높은 생체 적합성, 생체 활성, 골 전도성, 골 유도성, 무독성, 그리고 낮은 면역성 등과 같은 유용한 특성을 가지고 있는 것으로 보고 되었다. 또한, 돼지뼈, 소뼈, 생선 비늘, 생선뼈 등의 생체 폐기물이 낮은 가격으로 대량의 HA 생산을 위한 원료로 사용될 수 있다는 것이 널리 알려져 있다. 그러나 말뼈는 그 생산의 증가와 낮은 가격, 그리고 구제역으로부터 자유로움에도 불구하고, 거의 천연 수산화인회석의 생산을 위한

생물자원으로 사용되지 않았으며 제조 방법 또한 구성되지 않았다.

이 연구는 말뼈를 사용한 새로운 천연 인산 칼슘 생체물질의 생산을 위한 최적화된 방법을 제안하기 위해 수행되었다. 초기 생산공정은 이전의 돼지뼈를 대상으로 한 공정 (48시간 동안 과산화수소수에서 전처리 후 16시간 동안 1200 ℃에서 소결)을 참고로 하였다. 말뼈에서 유래한 인산 칼슘 생체물질의 특성은 서로 다른 뼈의 조직 유형 (즉, 경골과 해면골), 뼈 유형 (즉, 척추와 사골), 전처리 방법 (냉수, 과산화수소수, 온수), 소결 시간, 소결 온도에 따라 조사하였다. 또한, 더 넓은 의료 분야로의 적용을 위해 제작된 최종산물은 분말형으로 제작되어야 했으며, 이를 위해 습식 분쇄 (볼 밀) 및 건식 분쇄 (칼날 분쇄기)에 기반하여 분쇄 방법을 비교하였다. 생체재료로써 가공된 말뼈 가루의 잠재력을 평가하기 위해, 생체외 세포 시험이 합성된 HA 및 상용화된 소뼈 재료 (Bio-Oss)와 함께 MC3T3-E1 세포를 사용하여 수행 되었다. 수득한 말뼈 분말의 특성은 열중량 분석법 (TGA, X- 선 회절 분석법 (XRD), 푸리에 변환 적외선 분광법 (FT -IR), X 선 형광 분석법 (XRF), 그리고 전계 방출 주사 전자 현미경 검사법 (FE-SEM)으로 조사되었다. 그 결과 골조직과 골의 유형에 따른 차이는 나타나지 않았다. 또한, 전처리 방법에 따른 영향도 없었지만 처리 시간을 고려하면, 온수 방법이 좋았다. 소결 시간은 12시간으로 충분했으며, 600℃에 소결된 말뼈가 HA에 가장 가까운 XRD 피크를 보여주었지만, 1100℃ 에서 소결한 말뼈와 1300℃ 에서 소결한 말뼈가 각각 세포 독성과 증식에서 가장 좋은 결과를 보여주었다.

이 연구는 말뼈가 천연 인산 칼슘 생체소재로서 유망한 자원이 될 수 있으며 말 뼈 분말은 골 조직공학을 위한 생체소재로서 큰 잠재력을 가지고 있음을 보여주었다.

주 요 어: 골 대체재, 말뼈, 골 분말, 인산 칼슘 생체소재, 천연 수산화인회석, 골 조직공학.